DEGREE PROJECT IN CIVIL ENGINEERING AND URBAN MANAGEMENT,
SECOND CYCLE, 30 CREDITS
STOCKHOLM, *SWEDEN 2021*

Tunnel Seismic Prediction in Stockholm Bypass

MATILDA WESSÉN

JANITA ÖSTERBERG

KTH ROYAL INSTITUTE OF TECHNOLOGY
SCHOOL OF ARCHITECTURE AND THE BUILT ENVIRONMENT

TUNNEL SEISMIC PREDICTION IN STOCKHOLM BYPASS

MATILDA WESSÉN &

JANITA ÖSTERBERG

Master Thesis, 2021
KTH Royal Institute of Technology
School of Architecture and the Built Environment
Department of Civil and Architectural Engineering
Division of Soil and Rock Mechanics
SE-100 44, Stockholm, Sweden

© Janita Österberg & Matilda Wessén, 2021

Abstract

Tunnel Seismic Prediction (TSP) is a geophysical investigation method used to predict the rock conditions ahead of the tunnel face. The method has been used in different types of rock and rock conditions. The Swedish Transport Administration, Trafikverket, has used the investigation method in multiple locations in the large infrastructure project E4 The Stockholm Bypass. The method is however rather new to Swedish rock conditions, and there is therefore a need to evaluate the method to assess its strengths and weaknesses. In this thesis, the TSP method is compared to other investigation methods used in the Stockholm Bypass project at the location Sätra-Kungshatt where the tunnels cross underneath Lake Mälaren. The investigation methods include geological mapping and Measurement While Drilling (MWD). The TSP results are also compared to the engineering geological prognosis. An evaluation of how the seismic primary and secondary waves, V_p and V_s, correlates to rock quality was carried out, and a linear regression analysis was performed to determine if the wave velocities found using the TSP method correlate with the Q value retrieved through the geological mapping. It was found that the TSP method is capable of detecting weaker zones of rock mass, however no correlation between the wave velocities and the Q value used to describe the quality of the rock mass was found. When comparing the TSP results to the MWD results, it was found that the methods could be used as complements to each other as the different methods sometimes detected weakness zones where the other method did not. As the geology in this location of Stockholm Bypass overall was found to be complex with rather poor rock mass quality, it could be concluded that the TSP method might be better suited for less complex geology where the contrast in rock quality is greater.

Keywords
Tunnel Seismic Prediction, TSP, Seismic waves, Stockholm Bypass, Geological mapping, Measurement While Drilling.

Sammanfattning

Tunnel Seismic Prediction (TSP) är en geofysisk undersökningsmetod för att tillhandhålla en prognos av berget framför tunnelstuffen. Metoden har använts i olika typer av berg och bergförhållanden. I Sverige har metoden använts av Trafikverket vid flertalet tillfällen i infrastrukturprojektet E4 Förbifart Stockholm. Metoden är dock relativt ny för de svenska bergförhållandena, vilket gör att det finns ett behov av att utvärdera metodens styrkor och svagheter i dessa förhållanden. I detta masterprojekt har resultaten som tillhandahållits från TSP-metoden jämförts med resultat från andra undersökningsmetoder som använts vid vattenpassagen vid Sätra-Kungshatt där tunneln korsar under Mälaren. Dessa undersökningsmetoder inkluderar geologisk kartering och Measurement While Drilling (MWD). TSP-resultaten har även jämförts med den ingenjörsgeologiska prognosen för området. Vikt har lagts på hur den seismiska primärvågen, $V_{p,}$ och sekundärvågen, $V_{s,}$ förhåller sig till den karterade bergkvaliteten. En regressionsanalys har även utförts för att avgöra om resultaten från TSP-metoden korrelerar med resultaten från den geologiska karteringen. Jämförelsen mellan de olika undersökningsmetoderna visade på att TSP kan påvisa svaghetszoner i bergmassan. Dock kunde ingen korrelation mellan våghastigheterna och Q värdet påvisas. Jämförelsen mellan TSP och MWD visade att de båda metoderna generellt visade liknande resultat. Dock kunde vissa avvikelser mellan resultaten från metoderna hittas, vilket göra att metoderna skulle kunna användas som komplement till varandra. Detta då de olika metoderna ibland kunde identifiera svaghetszoner som den andra metoden inte kunde identifiera. De svåra geologiska förhållandena på platsen kan ha bidragit till att TSP-resultaten över lag är relativt svårtolkade, vilket gör att TSP-metoden möjligtvis är bättre lämpad för mindre komplexa bergförhållanden där kontrasten mellan bra och dålig bergkvalitet är tydligare.

Nyckelord
Tunnel Seismic Prediction, TSP, Seismiska vågor, Förbifart Stockholm, Bergkartering, Measurement While Drilling.

Preface

This thesis is the outcome of a master project at the Royal Institute of Technology, KTH, in Stockholm as part of the master's programs Civil and Architectural Engineering and Environmental Engineering and Sustainable Infrastructure. The thesis was carried out in collaboration with the Swedish Transport Administration, Trafikverket. Throughout the project we have been motivated by the interest in Tunnel Seismic Prediction and how it can predict geological conditions. Valuable knowledge about interpreting seismic waves and the work progress of a big scale infrastructure project has been learnt, but the course of action has not come without circumstances, the effect of COVID -19 has both limited and postponed some of the events. Anyhow, we hope to inform and widen the perspective of the use of seismic investigations in Swedish geological rock conditions and for the knowledge to assist in further research.

Lastly, we are very grateful for the sincere help from our KTH Academic supervisor, Carl Wersäll, and our supervisors from Trafikverket, Axel Bolin and Claes Mellqvist, that have provided us with the information, assistance, and guidance we needed to successfully complete this thesis. We would also like to thank Mathilda Nyzell and Gustav Dahl at AFRY for compiling the information regarding the geological mapping and the MWD results.

Stockholm, June 2021
Janita Österberg & Matilda Wessén

Nomenclature

Terminology

Profile	Part along the tunnel excavation.
Section	Cross section of a tunnel profile.
Trafikverket	Swedish Transport administration

Abbreviations

TSP	Tunnel Seismic Prediction
N	North
S	South
W	West
E	East
MWD	Measurement While Drilling
RMR	Rock Mass Rating
RQD	Rock Quality Designation
Q-value	Rock mass quality (range 10^{-3} to 10^{3})
Q_{Seis}	Seismic quality factor
Q_{c}	Normalised Q-value
Q_{base}	Q-value when disregarding the ratio between water seepage and the stress reduction factor
HT	Main tunnel
BP	Bypass tunnel
TBM	Tunnel boring machine
UCS	Uniaxial compressive strength

Greek Symbols

ρ	Density	[t/m^3]
υ	Poisson's ratio	[-]

Subscripts

E	Elastic moduli	[N/m^2]
G	Shear modulus	[N/m^2]
K	Bulk modulus	[N/m^2]
M	Constrained modulus	[N/m^2]
V	Velocity	[km/s]
V_{p}	P-wave seismic velocity	[km/s]
V_{s}	S-wave seismic velocity	[km/s]
R^2	Squared correlation coefficient	[-]

Table of contents

1. Introduction 3

1.1. Background 3

1.2. Aim and objectives 4

1.3. Delimitations and limitations 5

1.4. Disposition 6

2. Literature study 7

2.1. E4 The Stockholm Bypass 7

2.1.1. Rock properties in Stockholm 8

2.1.2. Geological conditions in the water passage at Sätra-Kungshatt 11

2.2. Seismic waves 11

2.2.1. Wave velocity in rock 12

2.2.2. V_p and Q-value 17

2.2.3. Summary of wave velocity 20

2.2.4. Suggestion of evaluation of V_p 21

2.3. Tunnel Seismic Prediction (TSP) 22

2.3.1. Operation and acquisition of TSP data 22

2.3.2. Evaluation of TSP data 25

2.3.3. Limitations related to TSP measurements 26

2.3.4. Previous research related to TSP 27

2.4. Investigation methods 29

2.4.1. Geological mapping of tunnels 30

2.4.2. Measurement While Drilling (MWD) 31

2.5. Rock mass classification systems 32

2.5.1. Rock quality designation (RQD) 32

2.5.2. Q system 32

2.5.3. Rock Mass Rating (RMR) 34

2.5.4. Limitations related to rock mass classification systems 35

3. Method 37

3.1. Engineering geological prognosis 37

3.2. Geological mapping 39

3.3. Measurement while drilling 40

3.4. TSP 303 40

3.5. Statistical analysis 42

4. Results 43

4.1. Engineering geological prognosis 43
4.2. TSP results 44
4.2.1. Main tunnel, HT202 45
4.2.2. Bypass tunnel, BP201 46
4.2.3. Bypass tunnel, BP202 48
4.3. Results from geological mapping 49
4.3.1. Overall geological conditions at Sätra-Kungshatt 49
4.3.2. Main tunnel, HT202 51
4.3.3. Bypass tunnel, BP201 52
4.3.4. Bypass tunnel, BP202 53
4.4. Results from MWD sampling 54
4.5. Comparison between TSP and engineering geological prognosis 56
4.6. Comparison between TSP and geological mapping 58
4.6.1. Main tunnel, HT202 58
4.6.2. Bypass tunnel, BP201 60
4.6.3. Bypass tunnel, BP202 62
4.7. Comparison between TSP and MWD 65
4.7.1. HT202 65
4.7.2. BP201 67
4.7.1. BP202 67
4.8. Statistical analysis 70
4.8.1. Comparison with correlations from earlier work 74
5. Discussion 76
6. Conclusion and further research 80
Further research 81
7. References 82
Appendix I – TSP data 87
Appendix II – Data from geological mapping 90

1. Introduction

1.1. Background

In tunnelling there are many uncertainties. This since the rock mass that is excavated often is heterogenous and anisotropic. To reduce the uncertainties related to the tunnel project different investigation methods can be used. The investigation methods used can be either destructive, e.g., core drilling, or non-destructive, e.g. geophysical methods. The choice of investigation method is typically dependent on the project related features and the ground conditions (Lindfors, et al., 2019). Time and cost constraints may also affect the choice of investigation method as geophysical methods generally are more cost and time efficient, while destructive methods often are more expensive and time consuming but have a higher accuracy (Esmailzadeh et al., 2018; Alimoradi et al., 2008).

An example of a non-destructive method that has been used in different projects is the Tunnel Seismic Prediction (TSP) system developed by Amberg Technologies (Li, et al., 2017). The TSP system is a seismic investigation method that uses the reflection of seismic waves on the geological structure ahead of the tunnel to predict the geometry and location of the structure (Amberg Technologies, 2020a). The seismic waves are generated by 24 charges placed in a line on one of the tunnel walls. The arrival time of the reflected waves are recorded using receivers placed on both tunnel walls. The method uses a 3D-velocity based migration and reflector extraction technology (3D-VMR) to determine the location and geometry of the structure ahead of the face (Amberg Technologies, 2020b). It is estimated that the technique can predict the geology up to 150 m ahead of the tunnel face, though in more crystalline rock conditions the prediction range can be up to 200 m (Amberg Technologies, 2020a).

The TSP system has been combined with different analysis tools to predict the geology ahead of the tunnel face. Esmailzadeh et al. (2018) found that a combination of statistical analysis and TSP could be used to predict the RMR value of the rock mass with an acceptable accuracy. Alimoradi et al. (2008), on the other hand, used a trained artificial neural network together with TSP to estimate the non-linear relationship between the TSP results and the RMR value of the rock mass. Shi et al., (2014) also found that an advance optimization method based on Fuzzy Analytic Hierarchy Process (FAHP) and TSP could be used to accurately predict the geological conditions.

The TSP system is rather new to Swedish rock conditions and has only been used by the Swedish Transport Administration, Trafikverket, since the beginning of 2020. The technique has been used in the large infrastructure project E4 The Stockholm Bypass, a 21 km long highway designed to redirect traffic from the inner parts of Stockholm city. The highway will be located both above ground and in tunnels. As the technique has only been used in Swedish rock conditions since the beginning of 2020, not many measurements with the technique have been performed. There is therefore a need to evaluate the technique for the Swedish conditions and compare the results from the TSP measurements with the results from other investigations, including the excavated rock. This to evaluate if the results generated from the TSP method align with the results retrieved from the other investigation methods as well as the engineering geological prognosis. Measurement While Drilling (MWD) has previously been used in these types of projects. The TSP technology is expected to be used as a complement to the investigation methods that are already in use today.

1.2. Aim and objectives

The aim of the thesis is to compare the results generated from the TSP method to other investigation methods used in E4 The Stockholm Bypass project as well as the engineering geological prognosis. This to evaluate how well the TSP results align with the results from other investigation

methods. By comparing the results from the different investigation methods, an evaluation of strengths and weaknesses of the TSP method can be carried out. The objectives are:

- Identify and evaluate how different rock properties affect wave velocity.
- Compare results from TSP measurements with results from the engineering geological prognosis, geological mapping and MWD measurements to assess strengths and weaknesses of the TSP method.
- Perform a statistical analysis to find correlations between TSP measurements and results from geological mapping.

1.3. Delimitations and limitations

Note that the data provided by Trafikverket has been produced out of production purposes to be able to determine and design a suitable support for the tunnel. The project is delimited to a few profiles of Stockholm Bypass, the main tunnel (HT202), and the two parallel bypass tunnels (BP201 and BP202) going under the lake Mälaren between Kungshatt and Sätra south of Stockholm. Only data from investigations within this tunnel stretch is compared but a literature study will review the main issues with the TSP technology, interpretation of geophysics and seismic in general to strengthen or weaken the thesis.

The data provided by Trafikverket did not include the Q_{base} value for all tunnel stretches considered, hence the Q-value was used. The Q_{base} value is used to characterize rock mass and might be more suitable for comparison with wave velocity since the Q value is reduced by factors such as overburden and direction of the tunnel.

TSP Ease program is used to calculate or interpret seismic data derived from the operation and several results can be achieved by filtering and processing the data but only one outcome will be evaluated. However, some comments are made regarding some operational issues with the program.

The project is limited by investigation methods carried out of a production point of view and with no intention for interference of the operation or results from the project. Hence, handed data is treated with care for bias and other errors.

1.4. Disposition

The first chapter introduces the research field and the aim and objectives of the thesis, while the second chapter presents the theory behind the case study, seismic waves with respect to rock quality, several investigation methods and rock mass classification systems. The third chapter describes the method used in the thesis to answer the objectives. The fourth chapter presents the results and is divided into several subchapters. In chapter four, the results from the different investigation methods and the engineering geological prognosis are presented, followed by a comparison between the TSP results and results from the various investigation methods used. Finally, a statistical analysis is presented where the wave velocities found using the TSP method are compared to the Q value retrieved from the geological mapping. The results are discussed in the fifth chapter while the sixth, and final, chapter concludes the findings of the thesis.

2. Literature study

The literature study will first review the geological conditions in Stockholm, in particular the water passage between Kungshatt and Sätra. The literature study will then touch on the field of seismic waves, its importance for geophysics and how the primary wave velocity (V_p) and rock mass quality corresponds to one another. Lastly, the study will focus on geological investigation methods, which include TSP, MWD, geological mapping and different rock mass classification systems.

2.1. E4 The Stockholm Bypass

E4 The Stockholm Bypass project is a large infrastructure project in Stockholm, aiming at connecting the southern and northern parts of Stockholm by tunnels outside of the inner city (Trafikverket, 2021). It is mainly carried out to redirect the traffic from the inner city and to reduce the vulnerability of the Stockholm traffic system. The project consists of a 21 km new highway connecting Kungens kurva in the south to Häggvik in the north. 18 out of 21 km of the highway will be located in tunnels, which will pass underneath Lake Mälaren in multiple locations. The tunnels are excavated using conventional drill and blast method. Excavation of the tunnels in the southern parts started in 2016 and the entire Stockholm Bypass project is estimated to be finished and open for traffic in 2030 (Trafikverket, 2019a).

In the southern parts, the Bypass passes beneath Sätra and the island Kungshatt in Lake Mälaren (Figure 1). The tunnels will have to pass beneath Lake Mälaren twice before reaching Lovön. The geology in this area is expected to be complex, as the tunnels have to pass a large regional weakness zone in Lake Mälaren (Trafikverket, 2019b). To gather

information regarding the geology, two bypass tunnels (BP201 and BP202) are excavated parallel to the two main tunnels in the passage beneath Lake Mälaren at Sätra-Kungshatt.

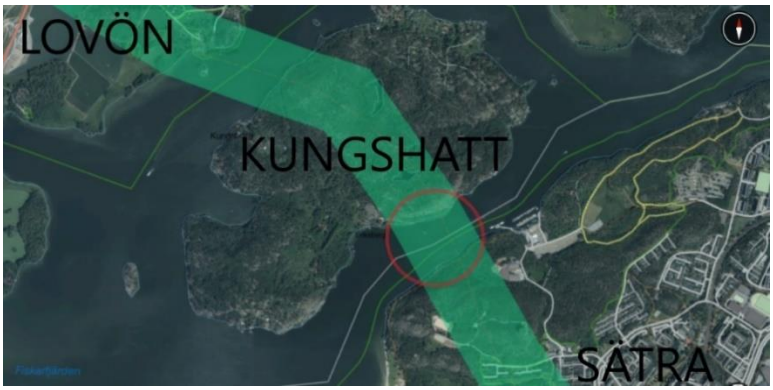

Figure 1. Location of tunnel excavation beneath Lake Mälaren between Sätra-Kungshatt, modified from SGU (2020).

2.1.1. Rock properties in Stockholm

The Swedish landscape has a history of glacial ice coverage, whereas the latest ended 10 000 years ago. The Ice regression has formed the landscape and left it with several typical formations such as polished boulders, glacial till, drumlins, eskers and lastly postglacial land uplift. Since the ice had a thickness of almost 1 kilometre it supressed the land beneath with its weight. While regressing, it relived the land that started to rise, it has risen several hundreds of metes and has several ten metres to go.

The geological conditions in Stockholm mainly features the result of the inland ice regression and a 1.8– 2.0 billion years old Svecokarelian orogeny. With regards to Stockholm Bypass, ice regression and orogeny is discussed mildly whereas plastic deformation zones are more elaborated.

The orogeny can be divided into several subgroups depending on differences in rock origin and chronological progress of structural, metamorphic features, nevertheless it can often be a parted by fracture zones or belts. The most distinct fracture belt in the region is 80 km long,

with its deformation zones creating series of belts in NE - SW directions, indicating compression in S - N directions (green arrows, Figure 2). Its conceptual movement under brittle reactivation can be found in Figure 2.

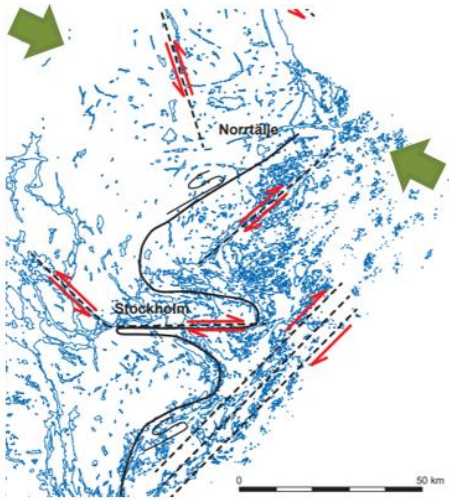

Figure 2. Fracture belt (SGU, 2018)

In the region of Stockholm, metasedimentary rock dominates the shallow depth with hints of metavolcanic and even small portions of sandstone. The content of quartz-feldspar and mica in metasedimentary rock is usually found as heavily altered and even partial melted resulting in mainly magmatic rock. Intrusive rock in the area is mainly composed of heavily altered and deformed granitoid, also known as metagranitoid. They are often rich in gneiss and transformed to veined gneiss. There is an abundance of quartz mineral that is common for metagranioid but regions with less quartz contents exist. Lastly, frequently occurring inclusions of metasedimentary rocks are common and elements of lightly scattered diabase and amphibolite occurs in the region (SGU, 2018).

Rock mass deformation mainly constitutes of plastic, brittle or brittle-ductile deformations. The plastic deformation is derived from very high temperatures and pressure, and covers regional areas as more concentrated zones e.g., plastic deformation zones. The more metamorphically transformed the rock is (which comes with higher

temperature, that in turn increases with depth), the more widespread the deformation is. Thus, the zones are more concentrated when created higher up in the crust. Brittle zones are created where the temperature is too low for plastic deformations to take place. These zones are often slimmer and distinct. Normally, they are very heterogenous and depending on its characterization it can stand as a hydraulic barrier. In the transitioning temperature brittle-ductile deformation is created.

Almost all rock is more or less heavily altered in the region, with the exception of some granite, diabase and the Jotnian stone of Mälaren. Plastic formation structures were formed under the Svecofennum orogeny, and new studies shows that they mainly include two phases of deformation. The first folding phase formed the previously mentioned metagranitoid, while the second phase resulted in reginal metamorphic calumniation.

The orientation of the structural planes and contact between them in the region varies depending on both the regional folding as well as the local folding. The regional folding is related to a larger folding, striking east in a s-shaped folding structure that is 80 km long. Some linear structures do however strike in one direction, with its lineation and folding axises tending to plunge steeply and towards northwest.

Heavy deformations zones are usually heterogenous in their distribution, the translation from the core of a deformation zone can vary significantly. This is important out of a geostructural point of view as excavating through this type of rock can mean interfering with good rock in one zone, and close to a plastic or brittle and fractured rock zone in another (SGU, 2018).

In a paper about 50 years of engineering experiences of geology and rock mechanics in Stockholm (SGU, 2018), reflects on rock stability, risk zones, rock tensions as well as geotechnical challenges. In terms on excavation in rock, the rock mass has often proven to be stable with only a few exceptions. The rock mass can often withstand large vertical loads but warnings signs rise with unfavorable fault planes, and even more when additional water in involved or if rock is slickensided, covered with mica, or graphite.

2.1.2. Geological conditions in the water passage at Sätra-Kungshatt

The geological conditions at the water passage at Sätra-Kungshatt are derived from both geological and geophysical studies using outcrop mapping, lineament interpretation, water-loss measurements, bore hole data and lastly drill core loggings. A report about factures in the area by Ignea (2015) showed presence and conditions of the main fractures to be steeply dipping in WSW-ENE and subordinate fractures of a set in NE-SW orientation. The main WSW-ENE fractures is in line with interpreted weakness zones with origin from the orogens, it also found to influence the water passage and includes deformation structures as example crushed rock or cataclastic rock. The subordinate NE-SW fractures may be highly underrepresented and could be a risk for tunnel stability. 33 zones of crushed rock and seven fracture networks were believed to have an influence on the planned tunnel between Sätra and Kungshatt. Lastly, investigations showed signs of undergone episodic reactivation in the area.

2.2. Seismic waves

Seismology is the study about earthquakes whereas seismic waves is the propagation of waves on and through the earth's surface. To understand how TSP works, it is necessary to address the basic knowledge about wave propagation in materials.

A rapid movement in one point causes transversal and horizontal movements in the particles of a medium in connection to a point or hypo centre. The movements of the particles in the medium will move around an equilibrium where it will return after the wave has passed. This movement can transfer energy for long distances. The velocity of a wave in perfect conditions for a confined body is determined by the elastic moduli E and rock mass density ρ, or more specific the bulk density of the material.

In a three-dimensional space only two kinds of waves can exist, the primary and secondary waves, or P-waves and S-waves, respectively. P-

waves propagates through a medium by compression and dilation of particles parallel to the direction of the wave motion. The P-wave is also the fastest of the two wave types. Its velocity depends on the constrained modulus M, by the relation in Equation 1.

$$V_p = \sqrt{M/\rho} \quad \text{(Eq. 1)}$$

S-waves on the other hand causes the particles to shear perpendicular to the direction of the wave motion, similar to a sinus wave. It is controlled by the shear modulus G, by Equation 2.

$$V_s = \sqrt{G/\rho} \quad \text{(Eq. 2)}$$

Sjogren (1984) suggested to use P-wave and S-waves data from seismic results in hard rock to interpret quality, while Barton (1991) argued that the quotient V_p/V_s can imply the rock mass quality, the Q-value. The dynamic Poisson's ratio v can be derived from this quote according to Equation 3.

$$V_p/V_s = \sqrt{2 - 2v/1 - 2v} \quad \text{(Eq. 3)}$$

Whereas $V_p/V_s \approx 3 \rightarrow v \approx 0.25$ for zero-porosity rock, though higher values often appear in unconsolidated soil or fault zones near the surface.

The seismic quality factor Q_{seis} should not be confused with the Q-value as Q_{seis} characterises the seismic attenuation. It is defined by the maximum energy stored during a cycle E_{max} and is divided by the change in energy loss ΔE by Equation 4, whereas the Q-value indicates the rock mass quality defined by the use of a rock mass classification system.

$$Q_{Seis} = 2\pi \times E_{max}/\Delta E. \quad \text{(Eq. 4)}$$

2.2.1. Wave velocity in rock

There have been many studies of how wave velocity corresponds to different rock parameters, here presenting a few regarding the P-wave.

In a study by Khandelwal (2012), investigating the correlation between the P-wave and the physio-mechanical properties from Indian rock samples of igneous, sedimentary, and metamorphic rock, strong linear relations were found for uniaxial compressive strength, density,

young's modulus and more. Poisson's ratio did however show a non-linear relationship. Figure 3 presents these relationships. Observing an increase in P-wave velocity along with increased compressive strength, density, young's modulus and Poisson's ratio.

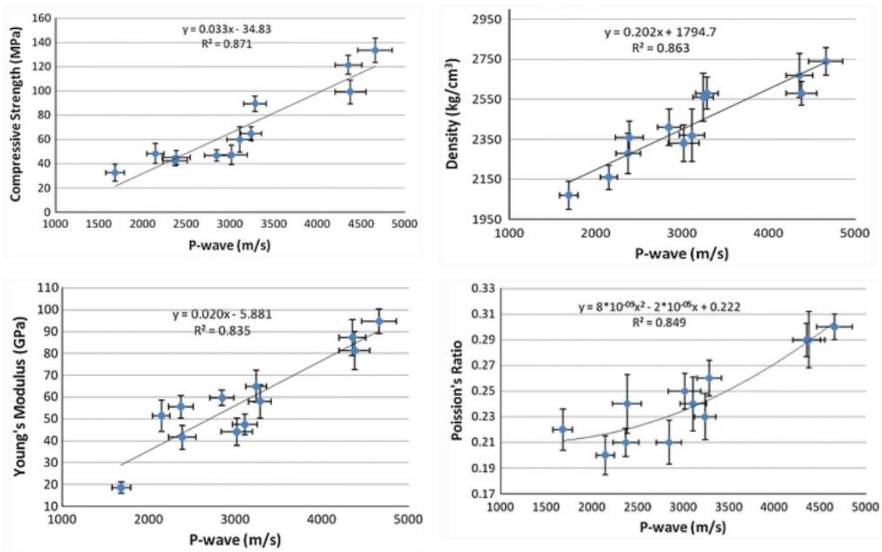

Figure 3: P-wave correlations with various rock parameters. Compiled from Khandelwal (2012).

A study by Kahraman (2001) investigated the relation between numbers of rock joints and V_p, indicating a linearity between increased jointing and decreased P-wave velocity. The study was carried out for a few block specimens (two Granite, three Travertine and one marble). The specimens were handpicked, and the joints were artificially created by sawing.

Barton (2006) emphasizes numerous of complications with using seismic methods. Some of them having to do with misinterpretation by overestimating or underestimating seismic data. When depth increases many rock features changes, normally joint stiffness, stress and pore pressure increases while permeability, clay content in joints, joint aperture and frequency decreases. It can be considered appropriate to

focus on low velocities and high permeability zones when trying to interpret seismic data. Too high waves velocities can on the other hand indicate hard rock which could mean frequent cutter changes when using TBM due to extensive wear and delaying the tunnelling project. The following table (Table 1) presents the general trend of the properties (Barton 2006).

Table 1: Trends of rock properties followed by increased depth.

	Increased	Decreased
With increased depth follows:	• Joint stiffness • Stress • Pore pressure	• Permeability • Clay content • Joint aperture

Wave velocity in rock is a function of rock properties. The rock is not a perfect elastic medium, it is almost always anisotropic of some degree. When waves propagate through a hard rock the velocity increases, while in soft rock, hollow sections, high porosity and fracturing the velocity decreases. The velocity can change widely for the same rock and locally within the rock. An example of this is sandstone where the P-wave velocity ranges from 1.8 to 4.8 km/s, depending on factors such as density, porosity, overburden pressure, saturation, cementation, clay content, etc. (Dondurur, 2018). Surveys on how to investigate V_p in different kind of rock has mostly been executed in shallow ground conditions.

An important feature for wave propagation through any material is the absorption of energy. High-speed layers can hide lower velocity layers right behind, resulting in loss of information for rock conditions and overestimating the results.

Figure 4 shows how wave velocity can differ in the same rock type. An increase in S-wave, bulk density (which is defined as *dry weight of rock/ soil per unit volume*), saturation, cementation and depth generally increases V_p while increase in pore pressure and porosity decreases V_p (Telford, 1990). Table 2 summarizes what is compiled from Figure 4 as a function of increased or decreased V_p.

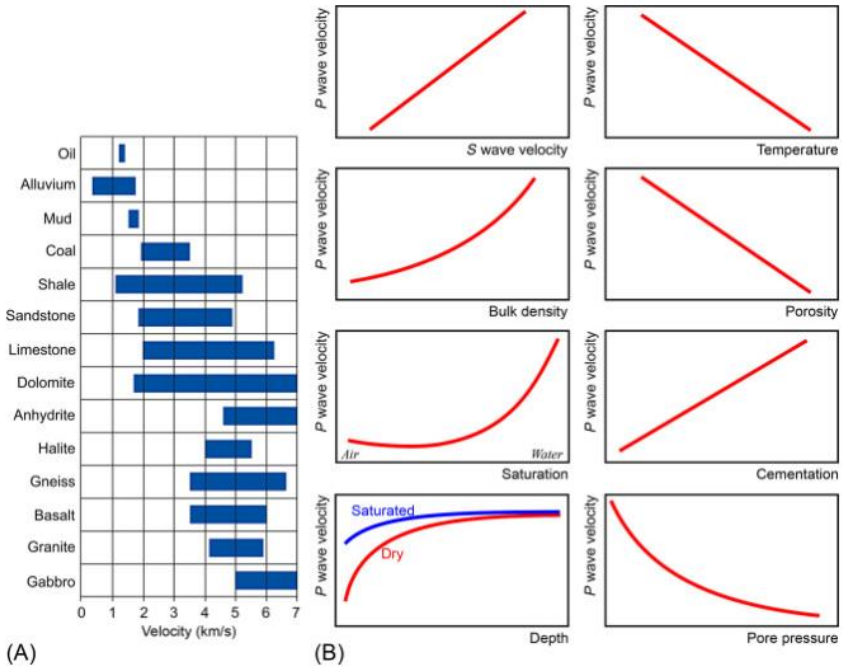

Figure 4: Compiled from Telford (1990).

A) P-wave velocity range of some specific rock types, and
(B) effect of different factors on P-wave velocity.

Table 2. Trends of V_p based on Figure 4.

Increased V_p follows by increased	○ Depth ○ Saturation ○ Bulk density ○ Cementation
Decreased V_p follows by increased	○ Pore pressure ○ Porosity ○ Temperature

Wang (2001) suggest that S-waves to the most part are not sensitive to changes in pore space and fluid content while P-waves shows sensitivity to saturation and type of fluid. Their ratio (V_p/V_s) can provide valuable information to distinguish lithology layers. Example for the case of soil or weathered rock horizons is that the water table can be detected by observing V_s remaining unchanged while V_p changes. This since shear waves, V_s, cannot respond to the water content due to its lack of shear stiffness (since it is liquid). When V_s also changes, a layer has been crossed (Barton, 2006).

Wave velocities tend to increase with depth, but this does not necessarily mean better rock quality, and can sometimes be misinterpreted as being better rock than reality proves, as the increase could be the result of higher rock stress (Barton, 2006). When encountering better rock quality along with an increase in V_p, the rock quality should suggestively be controlled continuously by core drilling or other investigation methods. In general, for hard rock the Q-value has shown to be ten-fold improved with 1 km/s in additional depth for a 50 m deep tunnel. Meaning that for a Q-value of 1 and V_p of 3.5 km/s near-surface to increase to V_p 5.5 km/s at depth, the Q value would more likely be 10 rather than 100, implied by a V_p equal to 5.5 km/s nearer the surface.

Apart from overburden, water depth is important for cases of completely dry undrained sub-aqueous tunnels. For the reason above, load of rock and water may give a false impression of rock quality at depth to an extent of 1 to 2 km/s.

Seen in many cases is that the foliation of bedding planes can cause significant velocity differences depending on angle of incidence to the foliation. In one case, parallel plane showing V_p of 5 km/s while perpendicular to the foliation showing 4 km/s (Barton, 2006). The same reasoning applies when joints or cracks are parallel, velocities are higher and less sensitive to stress level. Jointing in shear and fault zones has an increasing influence on Poisson's ratio and can overcome 0.4.

When the rock is weathered, the increase in void space can result in reduced velocities as water saturation decreases below 100 %, with

weathered rock the velocity reduction is not as altered or distinct. It may be several km/s due to increasing degree of fracturing and more often is this the case for near surface constructions. For unweathered hard rock condition, velocities at 5-6 km/s dominates. What may cause construction problem is lower velocities at 2.5 to 3.5 km/s that may be too fractured or indicate a weakness zone. But when observing these velocities for weaker and more porous rock (e.g., sandstone), the rock condition may be excellent. The point is that velocity says nothing per se about the rock condition but in contrast and relation to various background information the conditions can be interpreted more righteous.

In a study about wave propagation through filled joints, the P-wave velocity was found to be affected by joint properties, pre-stressed conditions, and input energy of the incident wave (Jianchun, Guowei, & Huang, 2010). Larger width and higher water content would reduce the P-wave velocity while pre-compressive stress would increase it. It was concluded that the presence of pre-stress could reduce the loss of incident P-wave velocity through a filled joint which was in line with another study by Selim and Ahmed (2006).

The interpretation of V_p can be difficult since it may be influenced by many factors such as seismic velocity, porosity, micro fractures, rock strength, density, depth, saturation, type of saturation fluid, joint frequency, and stress. The velocity also increases with depth, creating various out-puts of what V_p indicates. In addition, the operator and the set-up of a seismic device can have a significant impact on results. The most important aspect from an engineering perspective would be how to sort and evaluate among these factors. Common experiences as weathered rock and large fault width or open jointing has occurred, and as mentioned, the magnitude of hidden lower velocities layers and anisotropic stress, structure or bedding could be an additionally pitfall.

2.2.2. V_p and Q-value

There has been attempts made in intervals during the development of engineering geology and rock engineering to relate V_p to various rock

quality values as the Q-value or RQD. For several cases from hard rock tunnelling projects, a correlation between V_p and the Q-value was suggested by Barton (1991) (Equation 5), whereas V_p is given in km/s. By rearranging the equation, it can also be expressed as Equation 6, with Q ranging from 0.001 to 1000. The relation finds support from earlier work by Sjøgren (1979).

$$Q = 10^{(V_p - 3.5)} \quad \text{(Eq. 5)}$$

$$V_p = 3.5 + log\ Q \quad \text{(Eq. 6)}$$

Barton also suggested a specific correlation for Q-values in granite, Equation 7 expresses this relation.

$$Q = (V_p - 3600)/50 \quad \text{(Eq. 7)}$$

Later the correlation in Equation 5 was normalized using the uniaxial compressive strength σ_c (UCS), by Equation 8. The improved relationship now follows by Equation 9.

$$Q_c = Q \times (\frac{\sigma_c}{100}) \quad \text{(Eq. 8)}$$

$$V_p = 3.5 + log Q_c. \quad \text{(Eq. 9)}$$

The relation is shown in Figure 5 using correlation for porosity and for trial-and-error fitting for depth. Both low and high velocity rocks and with various porosity has been used in the trial (Barton, 2002). Rock samples including chalks from Israel, sandstones from China and Japan, granites and gneisses from Norway and more has been used for the test.

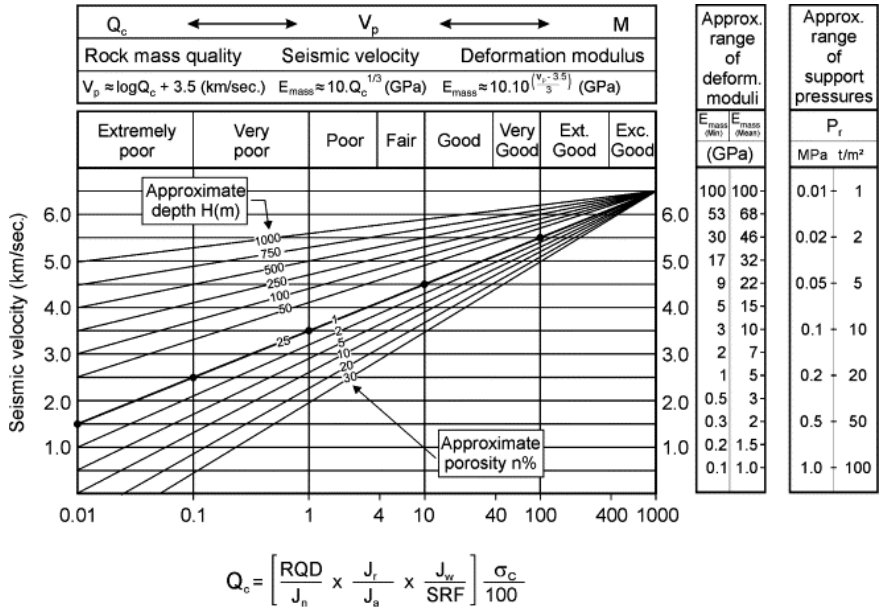

Figure 5: Integration of Q, V_p, σ_c, porosity, depth and static deformation modulus E_{mass}. Compiled from Barton (2002).

To illustrate how to use the methods, an example is given. Assume a tunnel 500 m down giving an V_p of 5.0 km/s, if neglecting the porosity (n%), the Q_c is 1.0 (Y-distance from the point where V_p=5 km/s crossing 500 m and the pointed thicker line). By rearranging the equation, the Q-value can be derived from Equation 8. To derive the Q-value, both porosity and uniaxial compressive strength has to be estimated.

A recent study concerning the use of TSP in several weakness zones in a partly subsea tunnel located at Mekjarvik, Norway, showed how P-wave velocities at 5000-6700 m/s obtained mapped Q-values around 10 for a geology dominated by gneiss and granite, (Figure 6) (Nordbø, 2020). These values were plotted against the correlation suggested by Barton (2002) along with relationships determined in studies by Eidesen (2013), Gjelsnes (2013) and Lausund (2015) for the same tunnel but for different locations and time. All resulting in higher Q-values than the mapped ones except for the correlation given by Laushand. For the green line (Barton,

2002) the UCS was determined to $Q_C = 282\,MPa$. However, the author concluded no significant relation between the linear correlation of the mapped Q-values and other presented relationships. By observing the linear correlation, a very low R^2 value is obtained indicating no correlation between the authors own mapped Q-values and V_p.

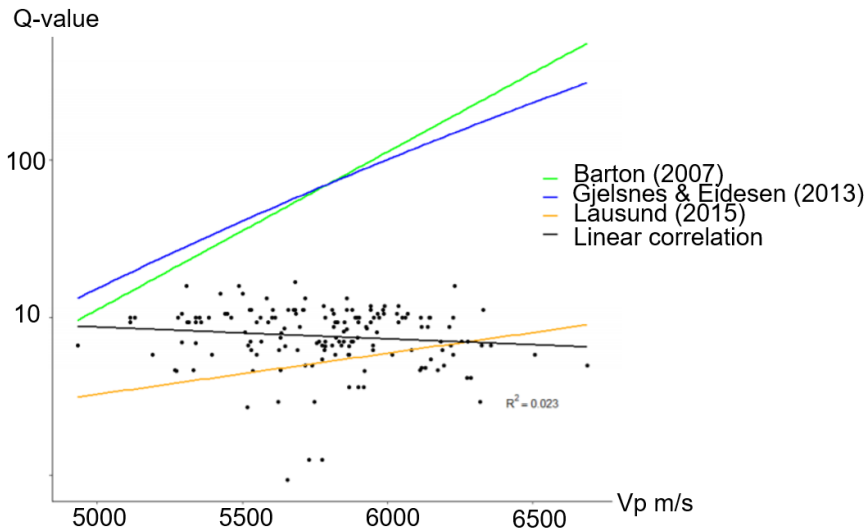

Figure 6: Norwegian study of Q-values against V_p using TSP. Compiled from Nordbø (2020).

2.2.3. Summary of wave velocity

A summary of what earlier studies have shown regarding the trend of V_p and its possible indications can be seen in Table 3.

Table 3. Possible indications for trends of V_p.

Trend of V_p	***Possible indication***
Increase	○ Increased Depth ○ Increased Saturation ○ Increased Bulk density ○ Increased Cementation ○ Parallel foliation planes ○ Pre compressive stress

Decrease	○ Decreased pore pressure ○ Decreased porosity or weathered rock ○ Decreased temperature ○ Perpendicular foliation planes

2.2.4. Suggestion of evaluation of V_p

The following notes is only a suggestion of how to evaluate V_p and associated mechanical properties based on previous studies regarding seismic investigation for rock engineering purposes. The following notes exclude random errors by the operator. Suggestively, the tunnel sequence should be divided into zones.

- Expected rock type.
  - As emphasised, seismic velocity is controlled by many factors and cannot define lithology by itself. The expected rock type should be identified and considered before drawing any conclusion of V_p. E.g. if hard rock is expected, for example granite, V_p should vary between 4 and 6 km/s.
  - Unfavourable rock conditions can be expected when facing values of V_p lower than expected for the rock, and the other way around.
- Water.
  - Indication of water appear when V_s remains constant while V_p changes since V_s does not respond to water content.
- Dynamic Poisson's ratio.
  - A high ratio can be an indication of fault and shear zones.
- Low velocities with high permeability.
  - Indication of bad rock for excavation purposes.
- Foliation planes.
  - Identify angle of incidence for foliation planes with other investigation methods. Care for parallel planes (with the excavation direction) since they are more difficult to

detect, leading to higher wave velocities that may be misleading.

- Q-value
    - The relationship between V_p and the Q-value is uncertain. Barton (1991) has suggested one relationship applied to granite (Equation 7) and the more general relationship in (Equation 6), that has been updated with respect to depth and porosity, see Figure 5.

2.3. Tunnel Seismic Prediction (TSP)

Tunnel Seismic Prediction (TSP) is a geophysical investigation method developed by Amberg Technologies, aiming at predicting the rock mass conditions ahead of the tunnel face (Amberg Technologies, 2020a). The technology is a seismic method that uses the reflection of the seismic waves on the geological structure ahead of the tunnel to estimate its location and dimensions. It is estimated that a prediction of up to 150-200 m ahead of the tunnel face can be provided. However, the accuracy of the prediction decreases as the distance from the tunnel face increases (Dickmann & Sander, 1996). In the Stockholm Bypass project, the TSP 303 system has been used. The operation and acquisition of data using this method is described below, as well as the evaluation of the gathered data. Finally, a description of the limitations related to the method is provided and previous research related to TSP is presented.

2.3.1. Operation and acquisition of TSP data

The seismic waves used to determine the quality of the rock ahead of the tunnel face are generated from 24 charges with a 1.5 m spacing located on one tunnel wall (Amberg Technologies, 2020a). Four receiver holes are placed behind the charge holes, two on each tunnel wall. The front two receivers are placed 15 m from the charge placed furthest away from the tunnel face, and the two back receivers are placed 5 m from the front receivers (Figure 7). When the charges are fired, the generated seismic waves will propagate through the rock mass and will, once they hit the

border between different geological structures, be reflected back to the receivers. The receivers are 3-component receivers that records the reflected wave field of compressional and shear waves in three spatial directions (Dickmann et al., 2016).

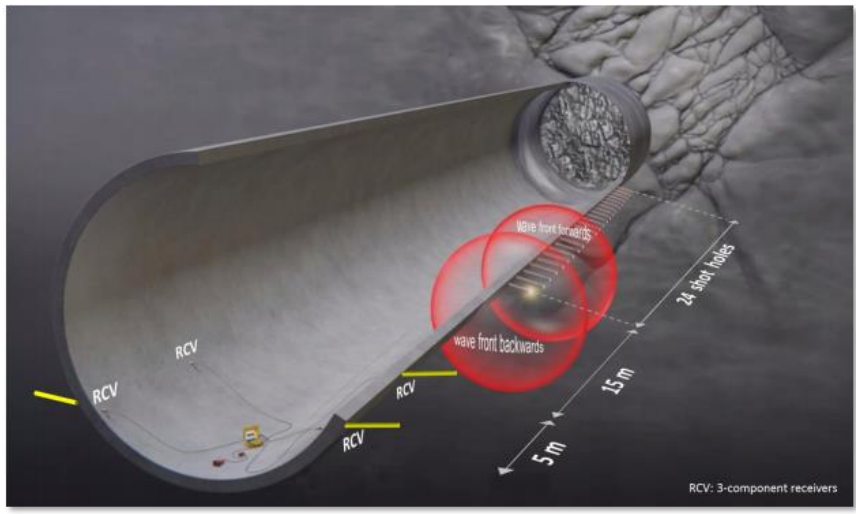

Figure 7. Overview of the measurement layout where four receivers (RCV) and 24 explosives are included. From Amberg Technologies (2019).

Different shot configurations can be used when firing the charges (Amberg Technologies, 2020a). The different configurations include either single shot acquisition or multiple shot acquisition. When using a single shot configuration (Figure 8), single shots are fired independently of each other. The single shot acquisition procedure is favourable to use in situations where the seismic response of the rock mass is still unknown. This since the amount of charge used can be adjusted between individual shots. When using the multiple shot acquisition procedure, the shots are divided into shot groups (Figure 9). Each shot group includes several shot holes that will be fired at the same time. Once the first shot group has been fired, the other shot groups will be fired one by one with an appropriate time delay. The number of shot holes included in one shot group can vary, however Amberg Technologies (2020a) recommend that

six shot holes per group should not be exceeded. It is common that a single test shot is fired before the shot groups to verify that the amount of charge used is correct. The advantage of using a multiple shot acquisition procedure is that the time of measurement is shorter, meaning less downtime in the tunnels.

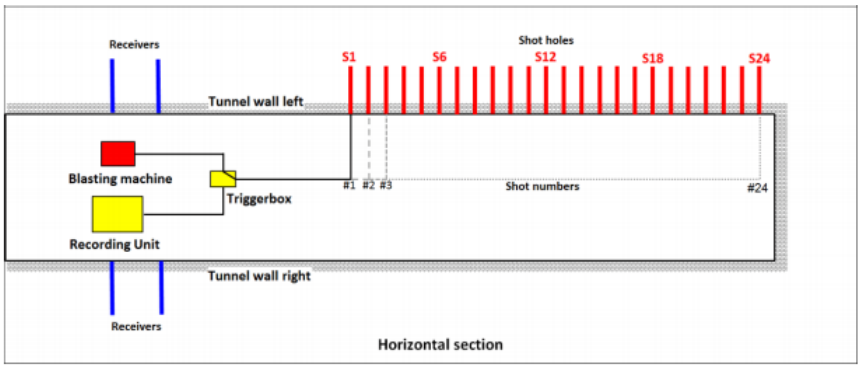

Figure 8. Measurement layout for single shot acquisition. From Amberg Technologies (2020a).

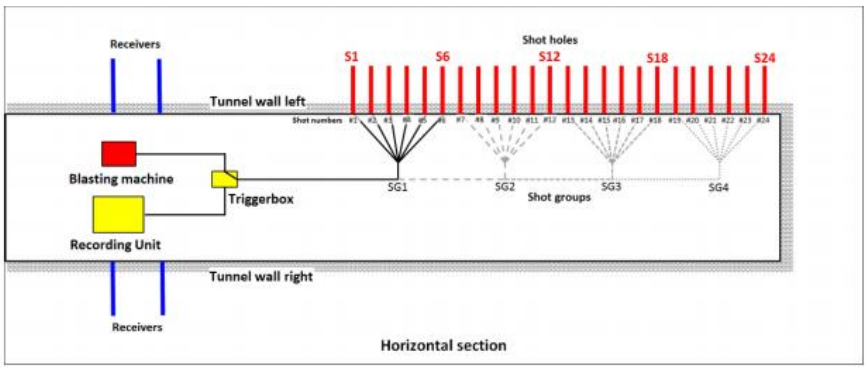

Figure 9. Example of a measurement layout for multiple shot acquisition. From Amberg Technologies (2020a).

2.3.2. Evaluation of TSP data

Once the data has been acquired it is processed in a computer software to extract the results. Amberg Technologies have developed a software called Amberg TSP Ease that uses a 3D-velocity based migration and reflector extraction technology, 3D-VMR, to generate 3D images of the geology ahead of the tunnel face (Amberg Technologies, 2020b). A detailed description of the procedure used to generate the results from the software could not be found, however a general overview of the procedure is provided. The 3D-VMR technology creates a velocity model by migrations with a known test velocity and an analysis of migration errors (Dickmann, 2014). The process is iterated until a final image computation gives the best fit model. Once the velocity model has been determined, the next step is to determine the most significant reflectors. Least-square-fit planes and their spatial locations are then computed using the reflectors. Mechanical properties such as Poisson's ratio and the Dynamic Young's modulus can then be calculated using Equation 10 and 11, respectively.

$$\mu = \frac{V_p^2 - 2V_s^2}{2\left(V_p^2 - V_s^2\right)} \qquad \text{(Eq. 10)}$$

$$E = \rho V_s^2 \left(\frac{3V_p^2 - 4V_s^2}{V_p^2 - V_s^2}\right) \qquad \text{(Eq. 11)}$$

Once the most significant reflectors have been determined and the velocities and mechanical properties have been calculated, the results are presented in graphs, 2D and 3D images. The generated graphs show the changes in the P- and S-wave velocities in front of the tunnel face, as well as the changes in the mechanical properties and the V_p/V_s ratio. The generated 2D and 3D figures show the reflectors found ahead of the tunnel face. In the 3D figures, 3D rendering can be chosen, which generates expected weakness zones and their expected shapes in 3D. In the 2D figures, the reflectors are shown together with a chosen parameter to be able to interpret and predict the geology. The chosen parameter can

be either a mechanical parameter, such as the Dynamic Young's modulus, or the P- or S-wave velocity. The 2D figures show a vertical point of view as well as horizontal point of view. This to be able to analyse the results from different angles with regards to the tunnel. The general idea when interpreting the results from the evaluation is that areas with a lower P- or S-wave velocity often are of a poorer rock mass quality than areas with a higher P- and S-wave velocity (Amberg Technologies, 2020b).

2.3.3. Limitations related to TSP measurements

As with any other geophysical investigation method there are uncertainties and limitations related to the TSP measurements. Overall, geophysical investigation methods are often seen as subjective as the results from the measurements require interpretation. A limitation related to TSP is, as previously mentioned, that the accuracy of the results from the TSP measurements decreases as the distance from the tunnel face increases (Dickmann & Sander, 1996). Dickmann and Sander (1996) have concluded that the prediction error in the location of geological structures for investigations with a range between 50-200 m can be up to 10%. Another limitation is the difficulty in accurately detecting geological structures not perpendicular to the tunnel axis (Li, et al., 2017; Lin & Li, 2014; Dickmann & Sander, 1996). The most accurate results from TSP measurements are generated when a structure is perpendicular to the tunnel. This since the seismic signals have a higher probability of being reflected back to the receivers in the tunnel. If the geological structures are angled in relation to the tunnel, there is a possibility that the signals will be reflected away from the receivers, meaning that the seismic signal cannot be detected (Li, et al., 2017). This also means that the TSP system has a hard time detecting structures parallel to the tunnel axis. Larger more regular structures are also easier to detect than smaller irregular structures. This since there is a higher possibility of the seismic signals hitting the structure if it is larger, while the more regular shape increases the possibility of the signals not scattering and therefore reduces the probability of the signals not being recorded by the receivers.

When it comes to more complex geology, Lu et al. (2020) have suggested a few modifications to the conventional TSP measurement layout to increase the accuracy of the results. They have found that using explosives on both tunnel walls, instead of on just one wall, gives a more accurate result from the TSP measurements. They also suggest that receivers can be installed closer to the tunnel face to reduce the distance from the receivers to the anomalies. This to increase imaging accuracy. Amberg Technologies (2020a) also suggests that a second shot line on the opposite tunnel wall can be used. This to gather more information regarding the geological conditions. However, they state that it is more economical to use a single shot line, and therefore two shot lines are only recommended for more complex geology.

As with most geophysical investigation methods, TSP measurements can be impacted by noise from the surroundings. The generated noise can disturb the seismic signals and may alter them, meaning that the accuracy of the results decreases (Amberg Technologies, 2020b). To increase the accuracy, as little activity as possible should occur at the time of the measurement.

2.3.4. Previous research related to TSP

The TSP technology has been widely used in many different rock conditions. Lin and Li (2014) have for example found that the TSP method could locate karstic caves and fracture zones in the Qiyueshan Tunnel in the Hubei province, China. However, they found that there could be errors in the predicted location of the karstic caves and fracture zones when comparing the TSP results to the actual conditions found during excavation. Similarly, Li et al. (2015) used the TSP method to detect karstic caves in the Shangjiawn Tunnel in the Hubei province, China. The results received using the TSP system were found to agree well with field observations during construction.

Another example is that Alimoradi et al. (2008) have used artificial neural networks (ANN) in the Cheshmeh Roozieh Water Supply Tunnel in Iran to predict the RMR values ahead of the tunnel face with the help of TSP data. In this area, the rock mass consisted of mainly sedimentary

rock with fault zones and other weakness zones crossing the tunnel. The predictions of the RMR values with the ANN method were found to be accurate the first 80 m ahead of the tunnel face. Shi et al. (2014) on the other hand have used a Fuzzy Analytic Hierarchy Process (FAHP) in combination with TSP to predict the quality of the surrounding rock mass in the Shimenya tunnel, China. The study found that the results generated from the method were in good agreement with the actual rock mass. However, they also found that the method has its limitations, with the main limitation being the inherent subjectiveness related to the FAHP-TSP method and the expert evaluation method. Furthermore, the distribution of weights is also carried out with a certain subjectiveness.

In metamorphic and igneous rock conditions, the TSP method has been used in multiple projects. Dickmann and Sander (1996) have for example used the method in two railroad tunnels in Switzerland. For these two tunnels, the TSP method was used to indicate fault zones and fracture zones, as well as water bearing zones. More recent publications where the TSP method has been used in hard rock conditions include for example a Metro tunnel in India where the rock mass consisted of quartz-rich schist (Choudhary & Dickmann, 2019), and a raw water transfer tunnel in Malaysia excavated in granite (Von & Ismail, 2017). For the Metro tunnel in India, TSP was used to detect an abandoned tunnel with an uncertain tunnel axis close to the new tunnel excavation. For the raw water tunnel in Malaysia, TSP measurements were used together with ANN to predict the quality of the rock mass ahead of the tunnel face. Similar to the publication by Alimoradi et al. (2008), Von and Ismail (2017) found that the combination of TSP data and ANN could successfully be used to predict the rock mass quality.

Esmailzadeh et al. (2018) have performed a statistical analysis of the TSP data acquired at the Seman Rooziyeh spring conveyance tunnel in Iran. The analysis showed that there was a weak linear correlation between the independent parameters retrieved from the TSP measurements and rock mass rating as a single-variable. However, they also found that a multi-variable nonlinear statistical model can be used to predict the RMR value with an acceptable accuracy.

Dickmann (2014) used the TSP system to detect the geology ahead of the tunnel face. The results were then verified by comparing the TSP results to a probe drilling that had previously been carried out. The study showed that the results retrieved from the TSP method are in good agreement with the geological probe drilling carried out on site. It also showed that the TSP method can predict faults and fractures zones.

A master thesis by Nordbø (2020) investigated the use of TSP in Rogfast, Norway, for a large tunnelling project, similar to this report. Complex and large weakness zones were predicted in hard gneiss and granite by investigation methods including MWD and by using TSP in 11 seismic campaigns. The method did not reveal all geological details and predicted more low velocity zones than what had been mapped in the tunnel. TSP is also limited by sub horizontal joints and weakness zones, the author also suggested that TSP must be used as a supplement to systematic investigation methods during construction. It shows difficulties in the use of complex geology and should only forecast geological structures that are simple and limited to what is considered most important features.

Studies that show a strong correlation between the Q values and the wave velocities derived from TSP 303 plus could not be found. This does not necessarily mean that a correlation does not exist, however it shows that more research is needed to determine if and how the wave velocities are related to the Q value.

Similar techniques to TSP are for example the True Reflection Tomography (TRT) technique developed by NSA Engineering Company (Otto et al., 2002), and the Tunnel Seismic Tomography (TST) technique developed by Y. Zhao, Chinese Academy of Sciences (Zhao et al., 2003). The common denominator is that all methods are developed as tunnel geological prediction methods based on seismic reflection.

2.4. Investigation methods

The following sections provide a description of some of the investigation methods used in the Stockholm Bypass project. The methods described

are especially relevant for the part of the tunnel going from Sätra to Kungshatt.

2.4.1. Geological mapping of tunnels

Geological mapping is carried out in tunnels to determine the quality of the rock mass. The results from the mapping are often used to provide a recommendation of appropriate support for the tunnel and are therefore carried out continuously as the tunnel face advances. The geological mapping typically includes a general description of the rock mass, a description of the discontinuities and a classification of the rock mass using rock mass classification systems. The procedure of geological mapping is often standardized. In Sweden, Trafikverket have provided general guidelines based on guidelines from the International Society for Rock Mechanics and Rock Engineering (ISRM) and the Swedish standard SS-EN ISO 14689-1:2004. The following description of what is included in the geological mapping is based on the general guidelines provided by Trafikverket (Lindfors, et al., 2019).

As previously mentioned, geological mapping typically includes a general description of the rock mass, a description of the discontinuities and a classification of the rock mass using rock mass classification systems (Lindfors, et al., 2019). The general description of the rock mass includes a description of the rock type, grain size, alteration, and structure of the rock mass, as well as the compressive strength of the rock mass. All of these parameters can be observed in the field. A description of the discontinuities found in the tunnel should be provided, which includes a description of orientation, persistence, aperture, infilling and weathering of the joints. The description also includes a description of the water inflow from the joints, as well as clay infilling. Larger weakness zones are noted and mapped. Finally, a rock mass classification can be performed based on the data gathered from the geological mapping. The principles of rock mass classification are described in section 2.5.

2.4.2. Measurement While Drilling (MWD)

Measurement While Drilling is a technology used to determine rock mass properties by collecting drill performance parameters such as speed of rotation, penetration rate, operational pressure etc. Its application has been useful in the mining industry since 1970 and the gathered information can provide drill and blast engineers with specific and useful improvements of excavation progress (Higgins & Segui, 2002). The technology was first presented in Sweden by Schunnesson (1996) and was initially used to determine rock mass designation (RQD) by interpreting the response data from the drilling in a tunnel project in the north of Sweden.

With a microprocessor-based drill monitoring equipment to collect parameters, an overview of the ground conditions can be derived. Information about rock hardness, weathering and fracturing can be provided (Schunnesson & Sturk, 1997). Even boundaries between different rock type and localization of ore is enabled with high accuracy and resolution.

Since the equipment is installed on the drill it does not disturb the production or occupy the tunnel face. Another advantage is that it only takes a few minutes to produce an analysis on an ordinary computer (Schunnesson, 1998). On the other hand, derived data have proven to be largely affected by the drill operator and for a modern drill rig the settings are adjusted automatically to prevent damage to the machine (Almquist & Hamrin, 1993). Additionally, Higgins and Segui (2002) argued that direct parameters mislead the indication of rock mass properties. An example is the penetration rate that is proportional with rock strength which, in turn, is dependent on features as voids, discontinuities, and fractures that directly will affect the penetration rate.

In a recent paper linked to the same project about MWD and how it is used to predict rock mass quality and support, van Eldert et al. (2019) showed clear correlation between mapped rock conditions and MWD findings. It showed that MWD technology could be used to fill the gap between uncertainties in pre investigations and mapping after excavation, creating a better foundation for deciding optimal support. Additionally,

the study showed a correlation between Q-value and the fracture index. Fracture index is derived from normalized penetration rate and rotational pressure, meaning the index can reflex heterogeneity of the rock mass. For construction of tunnels, it may be possible to use MWD to estimate required rock support.

2.5. Rock mass classification systems

Rock mass classification systems are commonly used to describe the quality of the rock mass in relation to the tunnel project. This to aid decision-making and to make communication between parties easier (Stille & Palmström, 2003). When performing the rock mass classification, the rock mass is divided into different rock classes depending on the characteristics of the rock mass and the project related features. The classes typically range from poor to good rock mass quality. Different parameters are included in the classification depending on the classification system used. The most frequently used classification systems are the Q system and the Rock Mass Rating (RMR) system (Stille & Palmström, 2003).

2.5.1. Rock quality designation (RQD)

A parameter that is included in both the Q system and the RMR system is the rock quality designation (RQD). The RQD value is used to describe the degree of fracturing of the rock mass using drill core logs (Palmström, 2005). The concept was developed by Deere (1963) and can be defined as the percentage of intact core log pieces longer than 10 cm in the total length of the core run (Equation 12).

$$RQD = \frac{\sum Length\ of\ core\ pieces > 10\ cm}{Total\ length\ of\ the\ core\ run} \times 100 \qquad \text{(Eq. 12)}$$

2.5.2. Q system

The Q system was first developed by Barton et al. (1974) to estimate rock support for tunnels. The system is based on six parameters, that together

are used to calculate the Q value of the rock mass. The following equation is used to calculate the Q value:

$$Q = \frac{RQD}{J_n} \times \frac{J_r}{J_a} \times \frac{J_w}{SRF} \quad \text{(Eq. 13)}$$

where RQD is the rock quality designation, J_n is the joint set number, J_r is the joint roughness number, J_a is the joint alteration factor, J_w is the joint water reduction factor and SRF is the stress reduction factor.

RQD is used as an estimation of the joint density in the rock mass, while J_n describes the number of joint sets in the rock mass. Together, the quotient between RQD and J_n represents the block size. J_r is an estimate of the roughness of the joints in the rock mass, while J_a represents the degree of alteration or filling in the joints. The quotient between J_r and J_a provides a description of the frictional characteristics of the rock mass. Finally, J_w represents the degree of water seepage, while the stress reduction factor (*SRF*) accounts for the loading on the tunnel (Barton et al., 1974). Once the Q value has been calculated, the rock mass can be classified into one of nine rock classes ranging from the value 0.001, exceptionally poor, to 1000, exceptionally good (Table 4). By relating the rock class to the characteristics of the tunnel, the needed tunnel support can be estimated.

Both classification and characterization of the rock mass can be done using the Q system (Barton, 2002). Classification of the rock mass refers to relating the characteristics of the rock mass to the project related features, while characterization of the rock mass refers to determining the characteristics of the rock mass itself. When characterizing the rock mass using the Q system the quotient containing the stress reduction factor (*SRF*) and the water seepage is set to 1 in Equation 14 (Lindfors, et al., 2019). The value received from the characterization is called Q_{base}.

Table 4. Rock classes according to the Q system (Barton et al., 1974).

Rock class	***Q***
Exceptionally poor	0.001-0.01
Extremely poor	0.01-0.1
Very poor	0.1-1
Poor	1-4
Fair	4-10
Good	10-40
Very good	40-100
Extremely good	100-400
Exceptionally good	400-1000

2.5.3. Rock Mass Rating (RMR)

The Rock Mass Rating (RMR) system was developed by Z.T. Bieniawski with the most recent update published in 1989 (Bieniawski, 1989). The system is based on six parameters which can be measured in the field. Some may also be obtained through borehole data. The following parameters are considered in the RMR system:

- Uniaxial compressive strength of the rock mass (r_1)
- RQD value (r_2)
- Spacing of discontinuities (r_3)
- Condition of discontinuities (r_4)
- Groundwater conditions (r_5)
- Orientation of discontinuities in relation to tunnel excavation (r_6)

The mentioned parameters are first rated individually and then summarized to form the final rating of the rock mass according to Equation 14 (Bieniawski, 1989). The final rating ranges from 0-100. Once the final rating has been done, the rock mass is categorized into one of five rock categories ranging from very poor to very good rock (Table 5).

$$RMR = r_1 + r_2 + r_3 + r_4 + r_5 + r_6 \qquad \text{(Eq. 14)}$$

The final RMR value can be used to estimate the stand-up time of the rock, as well as the rock mass properties. It is however important to note that a great deal of judgement is needed when applying the rock mass classification to support design (Stille & Palmström, 2003). As with the Q system, the RMR system can be used to determine the characteristics of the rock mass itself. The value related to the characterization is called RMR_{base} and can be determined by leaving out the correction for orientation of discontinuities in relation to the tunnel (r_6) in the final RMR value (Lindfors, et al., 2019).

Table 5. Rock classes according to the RMR system.

Rock class	***RMR value***
Very poor rock	<20
Poor rock	21-40
Fair rock	41-60
Good rock	61-80
Very good rock	81-100

2.5.4. Limitations related to rock mass classification systems

When applying rock mass classification systems to any excavation it is important to know the limitations of the classification systems. Palmström and Broch (2006) have, for example, pointed out some uncertainties and shortcomings related to the Q system. They argue that the Q system fails to take the stresses acting on the rock mass into proper consideration as the stress reduction factor (*SRF*) can be seen as a total stress parameter. They also point out that rock strength, joint orientation, joint size and joint persistence are not included in the classification.

There are also uncertainties and limitations related to the RQD value, which is used in both the Q system and the RMR system (Palmström, 2005). An example of a limitation related to the RQD value is the fact that the core will receive an RQD value of zero if all core pieces are 10 cm or less, and an RQD value of 100 if all core pieces are 11 cm or more. This would imply that the rock mass is either highly jointed and of very poor quality if the RQD value is zero, or that the rock mass is excellent and has

very few joints if the RQD value is 100. Another limitation related to the RQD value is the fact that the value is based on drill core logs. This means that the RQD value is dependent on the placement and direction of the borehole (Palmström, 2005).

The use of the classification systems, both the Q system and the RMR system, is mainly beneficial during the preliminary design of the tunnel. This since there usually is little information on the rock mass in this stage, which means that the rock mass classification systems can be useful in providing an overview of the characteristics of the rock mass (Palmström & Broch, 2006). However, more detailed investigations are needed for the final design (Stille & Palmström, 2003). Classification systems can be seen as subjective as the results are based mainly on observations (Palmström & Broch, 2006). The observations made are dependent on the person performing the classification, as different results and observations often are generated by different people examining the same stretch of a tunnel.

It is also important to note that classification systems cannot be used as the only design method in rock design. This due to the inherent uncertainties related to the classification systems. When using rock mass classification systems, it is important to have an understanding of the geological conditions at the site, such as rock mass composition, stress conditions and groundwater conditions (Palmström & Broch, 2006). This since none of the classification systems can take all ground conditions into consideration.

3. Method

The thesis is based on a case study of a tunnel stretch in the project Stockholm Bypass. The specific stretch of the tunnel is located south of Stockholm, between Sätra and Kungshatt. The evaluated tunnel stretch is the so called “Mälarpassage”, which is the part of the tunnel excavated beneath Lake Mälaren at Sätra-Kungshatt. The case study includes a part of the main tunnel, HT202, and the two bypass tunnels, BP201 and BP202. To understand the geological conditions at the site, different investigations have been carried out. An engineering geological prognosis was produced in 2015 to provide a prognosis of the expected geological conditions for the preliminary design of the tunnel. During excavation of the tunnel, investigation methods such as MWD, TSP and geological mapping have been used to reduce uncertainties. To answer the objectives of the thesis, the results generated from the TSP measurements at the tunnel stretch were compared to the engineering geological prognosis, geological mapping, and MWD measurements. The data used for the comparison was provided by Trafikverket. A statistical analysis was also carried out to determine if the Q values correlate with the wave velocities.

3.1. Engineering geological prognosis

An engineering geological prognosis was produced by ÅF Infrastructure on behalf of Trafikverket in 2015 (Arghe, 2015). The prognosis includes the southern parts of the Stockholm Bypass project, from Kungshatt to Kungens kurva. The investigation methods used to provide data and information regarding the geological conditions at this tunnel stretch includes core drilling, geological surface mapping, seismic reflection and

refraction surveys, as well as resistivity surveys. The case study included in this thesis focuses on the prognosis of the tunnel stretch going from Sätra to Kungshatt at tunnel meter 12 480 – 12 750.

At the tunnel stretch Sätra-Kungshatt, seismic reflection and refraction surveys, resistivity surveys, and core drilling have been carried out. The seismic investigation methods were used to determine the depth to the bedrock. The seismic refraction surveys were also used to characterize the rock mass and locate zones of low velocity as these may indicate fracture zones and poor rock mass quality. The refraction surveys were carried out at eight different lines in NNW-SSE direction.

Resistivity measurements were carried out in Lake Mälaren between Sätra and Kungshatt in 2012 by SGU. The measurements were carried out along the planned heading of the tunnel. Two measurement lines were located at the same location as the seismic refraction surveys. The resistivity measurements were used to located zones of poor rock mass, which is typically indicated by a lower resistivity.

In addition to the seismic surveys and the resistivity measurements, core drilling was performed in three locations related to this tunnel stretch. The drill cores extracted were characterized according to the Q-system. The strike and dip of the major fracture zones encountered in drill cores were also determined.

Based on the information provided by the above-mentioned investigation methods, a general description and prognosis of the expected geological conditions was provided in the engineering geological prognosis. The geology was divided into zones of similar geological properties to provide a prognosis of expected rock classes ranging from good to extremely poor rock (Table 6). The prognosis is used to aid the preliminary design of the tunnel and therefore the tunnel was divided into different support classes depending on the expected rock class. The support classes range from I to III, where I is the lowest support class, meaning the least amount of support, and III is the highest support class, meaning the most amount of support.

Table 6. Rock classes.

Rock class	***Rock quality***	***Q***
I	Good rock	>10
II	Acceptable rock	4 – 10
III	Poor rock	1 – 4
IV	Very poor rock	0.1 – 1
V	Extremely poor rock	<0.1

3.2. Geological mapping

Geological mapping of the tunnels is performed continuously as the tunnel excavation progresses. The procedure used during the geological mapping is standardized by Trafikverket (Lindfors, et al., 2019), and includes a general description of the rock mass, mapping and description of joints, and a characterization and classification of the rock mass using the Q-system. The information was used to determine the rock mass quality in order to choose the proper amount of support needed in the tunnel. Once the quality of the rock mass has been determined the tunnel stretch is divided into different support classes.

When performing the geological mapping, the dominating rock type is noted together with the grain size and the alteration of the rock mass. Furthermore, the structure of the rock mass is noted, as well as estimated compressive strength. For joints, the orientation, persistence, aperture, infilling of joints and water leakage is mapped. The extent of larger weakness zones is also noted. Once all parameters have been mapped, the results are used to characterize and classify the rock mass according to the Q-system.

3.3. Measurement while drilling

Measurement while drilling (MWD) applied for tunnels is a pre-investigation method used during the tunnel construction. By documenting the response from drilling parameters as penetration rate, rotational speed, operational pressure etc., valuable information about the rock mass can be collected (Schunnesson H. , 1996).

MWD measurements have been performed during excavation of both bypass tunnels (BP201 and BP202) and main tunnels (HT202) to gather information regarding the geological conditions ahead of the tunnel face. The measurements in the main tunnel HT202 covers MWD data of the tunnel meter 12 595 to 12 740, while the measurements in the bypass tunnel BP202 covers data for the tunnel meter 115 to 240. Finally, the MWD measurements in the bypass tunnel BP201 cover data of tunnel meter 150 to 270. MWD data is derived from the visualization program GPM+ and the results are shown in a figure where estimated rock strength and the location of fractures are presented.

3.4. TSP 303

Three TSP measurements were performed with the TSP 303 system at the location of the tunnel stretch at Sätra-Kungshatt. The measurements performed in the bypass tunnels BP201 and BP202 were carried out by Amberg Technologies February 5th, 2019. The third TSP measurement, in the main tunnel HT202, was carried out by Trafikverket February 18th, 2020 as part of a course given at Trafikverket regarding the TSP 303 system. The measurement layout for the TSP measurement for each of the tunnels is very similar. An example of a measurement layout can be seen in Figure 10 where the measurement layout for the tunnel BP202 is shown.

Though the tunnels have similar measurement layouts, different acquisition configurations have been used. For the measurement in BP201, multiple shot acquisition was used. The shot holes were divided into five different shot groups, with the first shot group being a single

shot (shot hole 1) used as a test shot to confirm that the correct amount of charge is used. For the measurement in BP202, single shot acquisition was used. For the HT202 tunnel, multiple shot acquisition was used, however the first six shot holes were triggered as single shots while the remaining 18 shot holes were divided into three shot groups with six shot holes in each group. Once the data had been acquired, it was processed in the software Amberg TSP Ease to separate the primary, secondary, and surface waves and to extract the encountered reflectors. Once the reflectors had been extracted, the P- and S-wave velocities and the mechanical properties of the rock mass were calculated.

To evaluate if the results from the TSP measurements coincide with the engineering geological prognosis, the results from the geological mapping and the MWD measurements, a comparison was made. The comparison was made for larger structural changes in the rock mass as it is irrelevant to go into detail. The results from the TSP measurements were divided into zones of similar rock quality, which in turn were compared to the engineering geological prognosis and the other investigation methods.

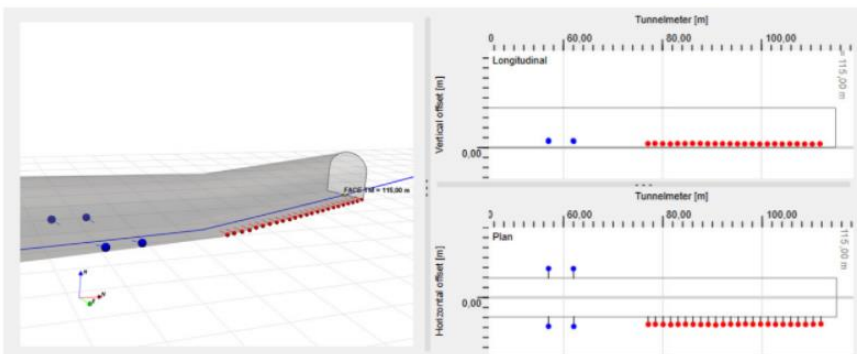

Figure 10. Measurement layout in the tunnel BP202. The blue dots represent the receivers while the red dots represent the shot holes.

3.5. Statistical analysis

A regression analysis was performed to determine if the results from the TSP measurements correlate with the results from the geological mapping. The P- and S-wave velocities from the TSP measurements were compared to the Q values retrieved from the geological mapping to determine the R^2-value. For areas where the Q values were presented in a span, an average Q value was used. In addition, an analysis between suggested relationship between Q-value and V_p by earlier work and retrieved Q values were compared.

4. Results

The results are presented from and in order; Engineering geological prognosis, TSP, Geological mapping and MWD, a comparison between the TSP results and engineering geological prognosis, geological mapping and MWD. Last presented is the statistical analysis.

4.1. Engineering geological prognosis

The results presented in this section are based on the prognosis presented in the engineering geological prognosis for the tunnel stretch at Sätra – Kungshatt (tunnel meter 12 480 – 12 750) (Arghe, 2015). This location is one of the locations where the tunnel crosses underneath Lake Mälaren. The rock cover for the tunnel is expected to be at least 25 m. The location is seen as a distinct weakness zone with a complex structure. The main weakness zone is expected to contain many different weakness zones with varying strike and dip. The main rock types found in the area are gneiss and granite.

In the southern parts of the tunnel stretch, towards Sätra, the main directions of the fractures are expected to be in an SSW-NNE and a W-E direction. The dip of the fractures is expected to be between S and E, which is in a direction towards Sätra. In the middle part of the tunnel stretch, the rock mass is expected to be heavily jointed. The main direction of the fractures is expected to be in a WSW-ENE direction, while the general dip of the fractures is expected to be in an NNW direction towards Kungshatt. The fractures in the northern parts of the tunnel stretch, towards Kungshatt, are expected to be located in the same direction as in the middle parts. The dip is also expected to generally be the same, however some fractures have a dip towards ESE. In the

northern parts, the number of fractures is expected to be less than in the middle and southern parts (Arghe, 2015).

In Table 7, a prognosis of the expected rock class for different parts of the tunnel stretch is presented. The prognosis is provided in the engineering geological prognosis to provide information regarding the geological conditions for the preliminary design. The rock is dived into five different rock classes (I-V) ranging from good to extremely poor rock (Table 6). The rock mass quality at Sätra-Kungshatt is expected to be poor with the most common rock classes expected to be very poor and extremely poor rock.

Table 7. Expected rock class of different parts of the tunnel located between Sätra and Kungshatt.

Tunnel meter	***Rock class***	***Q***
12 465 – 12 502 (Sätra)	Extremely poor (V)	0.1 – 1
12 502 - 12 510	Very poor (IV)	0.1 – 1
12 510 – 12 550	Extremely poor (V)	< 0.1
12 550 – 12 580	Very poor (IV)	0.1 – 1
12 580 – 12 610	Extremely poor (V)	< 0.1
12 610 – 12 650	Very poor (IV)	0.1 – 1
12 650 – 12 700	Poor (III)	1 – 4
12 700 – 12 980 (Kungshatt)	Good (I)	> 10

4.2. TSP results

The following section includes the results from the TSP measurements at the tunnels HT202, BP201 and BP202. The primary and secondary wave velocity is presented for each tunnel, as well as other parameters such as Poisson's ratio and the Dynamic Young's modulus. Poisson's ratio and the Dynamic Young's modulus are calculated according to Equation 10 and 11. An interpretation of the TSP results made by Trafikverket and Amberg Technologies is also provided. All results presented in this section are

taken from the reports written by Amberg Technologies (2019) and Trafikverket (2020) after the TSP measurements had taken place in the respective tunnels. More detailed TSP data can be found in Appendix I.

4.2.1. Main tunnel, HT202

The TSP results generated for the tunnel HT202 at Sätra-Kungshatt are presented in Figure 11. The tunnel stretch was divided into seven different areas depending on the properties of the rock. An interpretation of the TSP results can be found in Table 8.

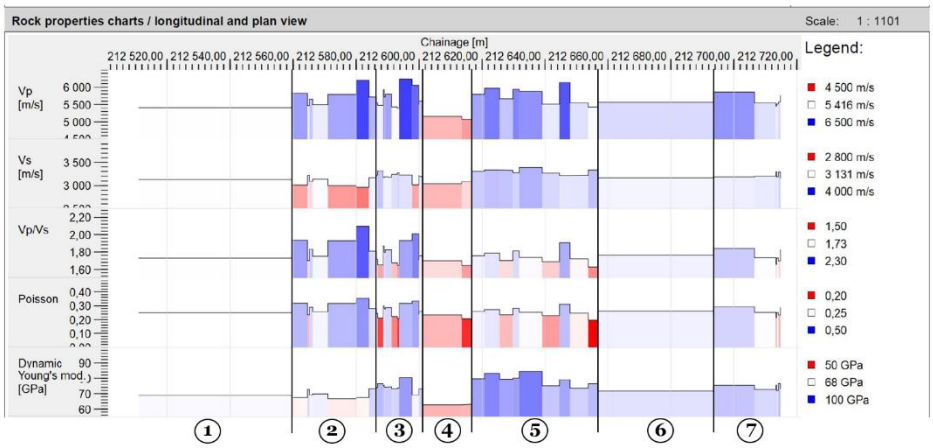

Figure 11. Results generated from the TSP measurement at HT202.

Table 8. Interpretation of the TSP results at HT202.

Area	*Tunnel meter*	*TSP interpretation*
1	- 12 584	Known rock conditions in already excavated rock. Reference level for wave velocity.
2	12 584 – 12 610	Uncertain assessment due to influenced from tunnel. Tunnel face located at 12 592. Varying rock quality.
3	12 610 – 12 626	Marginal improvement in rock quality compared to area 2. However, the rock quality is found to vary, meaning that a heterogeneous rock mass is expected.
4	12 626– 12 643	Homogenous area with worse rock mass quality than area 2 and 3. Potential weakness zone.
5	12 643 – 12 682	Heterogenous area with an overall better rock quality than area 4. Rock mass quality comparable to area 3.
6	12 682 – 12 719	Homogeneous area with average rock mass quality.
7	12 719 – 12 737	Area with better rock mass quality than area 6. However, the distance from the tunnel face is significant, meaning that assessment is uncertain. Possible influence from connections for bypass tunnels.

4.2.2. Bypass tunnel, BP201

In Figure 12, the TSP results for the tunnel BP201 are presented. The tunnel stretch was divided into seven areas depending on the properties of the rock. An interpretation of the results for each area can be found in Table 9.

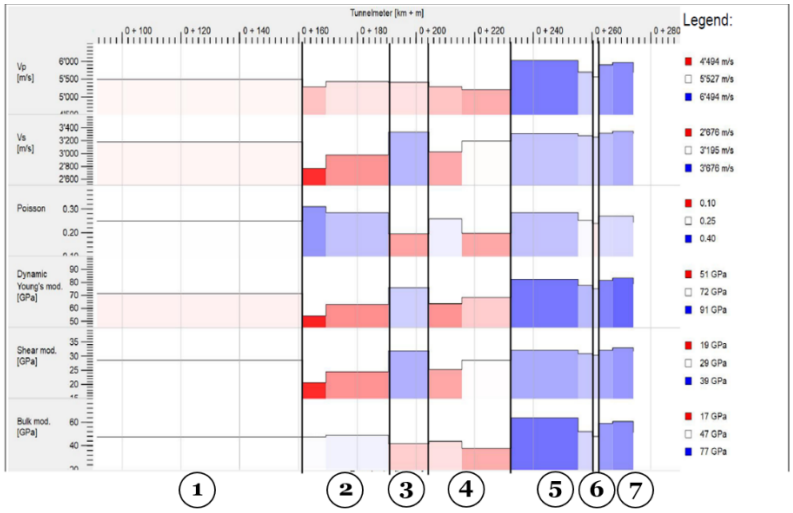

Figure 12. Results generated from the TSP measurement at BP201.

Table 9. Interpretation of the TSP results at BP201.

Area	***Tunnel meter***	***TSP interpretation***
1	– 161	Moderate to fair gneiss. Used as reference level.
2	161 – 191	Weakness zone. Possible water bearing zone.
3	191 – 204	Increased rock stiffness. Competent rock with less fracturing.
4	204 – 232	Decreased rock stiffness. Weakness zone.
5	232 – 260	Increased rock stiffness. More competent rock. Better rock mass quality than area 1, 2, 3 and 4.
6	260 – 262	Slight decrease in rock stiffness. Fair gneiss. Better rock mass quality than area 1, 2 and 4. Slightly worse rock mass quality than area 5. Comparable to area 3.
7	262 – 274	Increased rock stiffness. Competent gneiss. Rock mass quality comparable to area 5.

4.2.3. Bypass tunnel, BP202

The TSP results generated for BP202 are presented in Figure 13. The results were divided into eight different areas depending on properties of the rock. An interpretation of the results can be found in Table 10.

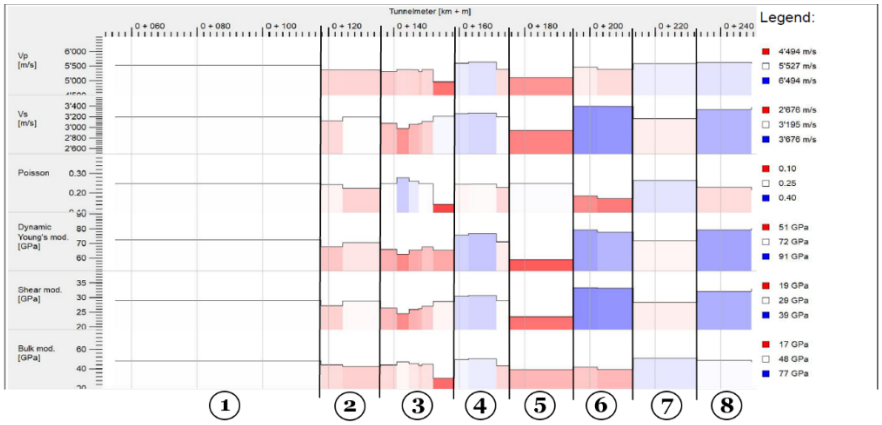

Figure 13. Results generated from the TSP measurement at BP202.

Table 10. Interpretation of the TSP results at BP202.

Area	***Tunnel meter***	***TSP interpretation***
1	– 118	Fair gneiss. Used as reference level.
2	118 – 136	Slight decrease in rock stiffness.
3	136 – 159	Further decrease in rock stiffness. Weakness zone.
4	159 – 175	Increase in rock stiffness. More competent rock. Better rock mass quality than area 1, 2 and 3.
5	175 – 195	Decrease in rock stiffness. Worse rock mass quality than area 1, 2 and 3. Potential weakness zone.
6	195 – 213	Increase in rock stiffness. More competent rock.
7	213 – 233	Slight decrease in rock stiffness. Fair rock.
8	233 – 250	Increase of rock stiffness. More competent rock. Comparable to area 6.

4.3. Results from geological mapping

The results generated from the geological mapping of the tunnels after excavation are presented below. An overall description of the geological conditions is presented followed by the rock classes and *Q* values determined for the three tunnels HT202, BP201 and BP202 at Sätra-Kungshatt. Data regarding the geological mapping is presented in Appendix II.

4.3.1. Overall geological conditions at Sätra-Kungshatt

Geological data of the tunnels HT202, BP201 and BP202 was provided by Trafikverket. The following section concerns a summary of the geology in the passage at Sätra-Kungshatt. The most commonly occurring rock types in the area are gneiss and sedimentary gneiss with intrusions of granite. The geologist has identified two large weakness zones and two more parallel to the excavation direction. The weakness zones follow the direction of Lake Mälaren and are parallel to the foliation of the sedimentary gneiss striking NE (020-050°). An overview of the structures found at the passage is presented in Figure 14 showing two large weakness zones and two smaller weakness zones in a light red colour.

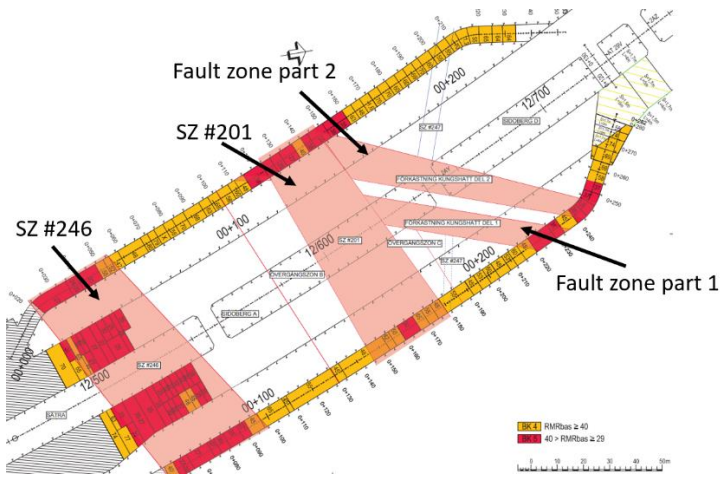

Figure 14. Overview of the structures found at Sätra-Kungshatt. Despite low resolution, identified weakness zones can be observed in light red colour.

The first weakness zone (zone 246) is located nearby Sätra and includes two heavily altered graphite plane structures with high clay content surrounding a 24-32 m zone of plastic and brittle sedimentary gneiss. The southern border of the weakness zone is distinct and has a strike towards NE (040-060°) and a dip towards SE. The northern border is not as distinct with a 4-11 m wide transitional zone with an approximately NE (030-050°) strike and a dip towards SE. The rock mass in the weakness zone consists of sedimentary gneiss with brittle deformation. Its foliation is heavily weathered and in times porous. Weakness zone 246 is believed to be prone to reactivation due to cementation, jointing and alteration of the rock mass. Granite intrusions can be found, which at times are water bearing and hydrothermally altered, which is a metamorphic process where the rock or its minerals is exchanged for water aqueous solutions.

The second weakness zone (zone 201) is mostly altered into graphite with infillings of clay in larger joints. The alteration decreases towards the north where breccia occurs. The zone includes less weathered and deformed quartz rich blocks, lenses of granite and sedimentary gneisses altered into K-feldspar. Plastic deformation has also been identified in the form of jointed granite parallel to the larger joints. Weakness zone 201 ends in a large clay filled joint with slices of sedimentary gneiss and occasional granite faults and alteration of k-feldspar.

Two fault zones (fault zone part 1 & 2) were identified parallel to each other with tens of meter in between. The first part consists of two clay filled graphite altered joints and less deformed blocks in a branched structure of two clay filled steep joints striking NE (030-050°) and dipping SE (70°) whereas one joint border jointed and blocky mica rich gneiss. Some translation and rotation of granite blocks has been noted, together with water bearing zones. The second part is similar to the first, with jointed rock with clay infilling and lenses of graphite altered sedimentary gneiss striking N (10°) and dipping E (70°). In addition, a blocky, K-feldspar altered, granitic intrusion was found. A water bearing zone was found in the main tunnel.

The remaining rock, besides weakness and fault zones, consists of a mixture of jointed sedimentary gneiss, quarts rich gneiss and granite intrusions together with altered K-feldspar. The main tunnels cross a third weakness zone (zone 247) however its boundaries are diffuse. The rock mass in zone 247 consists of sedimentary gneiss that is jointed, blocky, rich in mica and contains K-feldspar altered granite intrusions. Some clay filled contacts have also been identified.

4.3.2. Main tunnel, HT202

The rock classes and *Q* values determined after excavation of the main tunnel HT202 at Sätra-Kungshatt are presented in Table 11. The determined rock classes were found to vary from acceptable to extremely poor rock mass, with the most common rock classes being poor and very poor rock mass. A zone of extremely poor rock mass was found at tunnel meter 12 607 – 12 632, which indicates a larger weakness zone. However, as the entire area was mainly found to be of poor rock mass quality, this indicates that the entire area consists of a large weakness zone of varying quality as expected in the engineering geological prognosis.

Table 11. Rock class and Q values determined for the main tunnel HT202 at Sätra-Kungshatt (tunnel meter 12 567 – 12 742).

Tunnel meter	***Rock class***	***Q***
12 567 – 12 589	Poor (III)	1 – 3.9
12 589 – 12 593	Good/Acceptable (I/II)	3.6 – 12.5
12 593 – 12 597	Poor (III)	1.6 – 3.6
12 597 – 12 607	Poor/Very poor (III/IV)	0.2 – 3.3
12 607 – 12 632	Extremely poor (V)	0.02 – 0.1
12 632 – 12 642	Very poor (IV)	0.15 – 0.3
12 642 – 12 646	Poor (III)	1.7
12 646 – 12 666	Very poor (IV)	0.7 – 0.9
12 666 – 12 672	Poor (III)	2.5
12 672 – 12 678	Very poor (IV)	0.9
12 678 – 12 742	Poor (III)	1.1 – 3.6

4.3.3. Bypass tunnel, BP201

The rock classes and *Q* values determined after excavation of the bypass tunnel BP201 are presented in Table 12. The rock mass was found to be of poor quality throughout, with the most common rock classes being poor and very poor rock mass. The rock mass was found to be of extremely poor quality at both tunnel meter 160 – 167 and 220 – 229. At tunnel meter 259 – 263, the rock mass was found to be of good quality.

Table 12. Rock class and Q values determined for the bypass tunnel BP201 at Sätra-Kungshatt (tunnel meter 160 – 263).

Tunnel meter	***Rock class***	***Q***
160 – 167	Extremely poor (V)	0.04 – 0.06
167 – 175	Poor (III)	1.25 – 1.67
175 – 179	Very poor (IV)	0.19
179 – 191	Poor (III)	1.46 – 1.94
191 – 195	Very poor (IV)	0.31
195 – 203	Poor (III)	1.25 – 1.67
203 – 208	Very poor (IV)	0.16
208 – 220	Poor (III)	1.04 – 1.67
220 – 229	Extremely poor (V)	0.07
229 – 255	Very poor (IV)	0.1 – 0.4
255 – 259	Poor (III)	2.71
259 – 263	Good (I)	11.25

4.3.4. Bypass tunnel, BP202

The rock classes and *Q* values determined after excavation of the bypass tunnel BP202 are presented in Table 13. The quality of the rock mass was found to vary between acceptable and extremely poor rock mass, with the most common rock classes being poor and very poor rock mass. At tunnel meter 127 – 141, the rock mass was found to be of extremely poor quality which indicates a weakness zone. Rock mass of extremely poor quality was also found at tunnel meter 144 – 151. Rock mass of acceptable quality could be found at tunnel meter 172 – 180, 192 – 195, and 225 – 229.

Table 13. Rock class and *Q* values determined for the bypass tunnel BP202 at Sätra-Kungshatt (tunnel meter 115 – 248).

Tunnel meter	***Rock class***	***Q***
115 – 127	Very poor (IV)	0.11 – 0.7
127 – 141	Extremely poor (V)	0.02 – 0.06
141 – 144	Very poor (IV)	0.15
144 – 151	Extremely poor (V)	0.07
151 – 160	Very poor (IV)	0.2 – 0.21
160 – 164	Poor (III)	3.75
164 – 172	Very poor (IV)	0.25 – 0.33
172 – 180	Acceptable (II)	6.25
180 – 192	Poor (III)	2.57 – 3.7
192 – 195	Acceptable (II)	8.33
195 – 200	Poor (III)	1.9
200 – 204	Very poor (IV)	0.76
204 – 225	Poor (III)	1.25 – 3.33
225 – 229	Acceptable (II)	6.67
229 – 248	Poor (III)	1.48 – 2.22

4.4. Results from MWD sampling

MWD sampling were performed in all tunnel sections prior to excavation. An overview of the MWD results found at the passage between Sätra and Kungshatt can be seen in Figure 15. The figure shows the rock strength measured at the location. In the figure, north is approximately located upwards. Areas marked in red, yellow, and light green represents areas with lower rock strength. Potential weakness zones are marked in red. In the bypass tunnel BP202, the rock strength is expected to vary. A potential weakness zone is located at approximately tunnel meter 120 – 140 and crosses the tunnel in an approximately W-E direction (Zone A). The same weakness zone can also be seen in the tunnel HT202. Another potential weakness zone can be spotted that crosses the tunnels in a NE-SW direction north of the previously mentioned weakness zone (Zone B). Further to the north, an additional two potential weakness zone crosses the tunnels in approximately the same direction as the previous weakness zones (Zone C and D).

Similar to the tunnel BP202, the rock strength in the tunnel HT202 is expected to vary. A similar pattern to the weakness zones spotted in the tunnel BP202 can be seen for the tunnel HT202. Further to the north in the tunnel, the rock mass strength is expected to be better than to the south. For the tunnel BP201, the rock strength is also expected to vary, however the rock strength is expected to be better than for the previously mentioned tunnels. The weakness zones are not as distinct in this tunnel as for the other tunnels, however indications of the weakness zones can be seen.

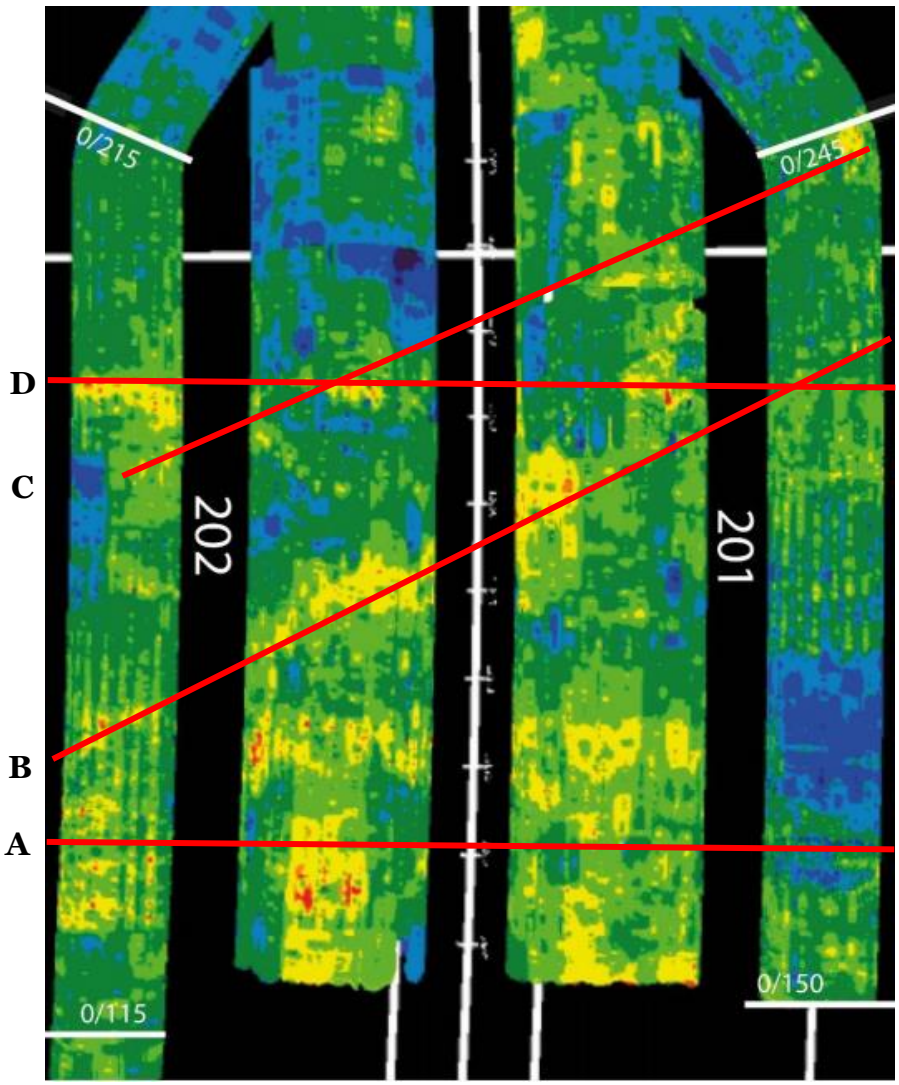

Figure 15. Overview of the MWD results (rock strength) found at the passage Sätra-Kungshatt. The bypass tunnel BP202 is located to the far left in the figure with the main tunnel HT202 located next to BP202. The bypass tunnel BP201 is located to the far right in the figure. Areas with lower rock strength are marked in red, yellow, and light green with red being the lowest rock strength. North is approximately located upwards. Potential weakness zones are marked in red.

4.5. Comparison between TSP and engineering geological prognosis

A comparison between the results generated from the TSP measurement at HT202 and the engineering geological prognosis was carried out to determine if the results coincide (Table 14). By looking at the results generated from the TSP measurement in HT202 (Figure 11) and the comparison with the prognosis in Table 14, one can conclude that the prognosis and the results from the TSP measurement show similarities. A few discrepancies between the prognosis and the TSP results can however also be seen, with the first being at tunnel meter 12 584 – 12 610 (Area 2) where the prognosis expects the rock mass to be extremely poor, while the TSP measurements show a rock mass quality similar to tunnel meter 12 610 – 12 626 (Area 3) which is expected to be of very poor quality. The TSP assessment for area 2 is however deemed to be uncertain due to influence from the already excavated tunnels.

Another discrepancy can be found at tunnel meter 12 626 – 12 643 (Area 4) where the TSP results deems the rock mass quality to be worse than area 2 and 3, but the prognosis expects the rock mass to be of very poor quality which is comparable to area 3. Another discrepancy to note is that the rock mass quality at tunnel meter 12 682 – 12 719 (Area 6) from the prognosis is expected to vary from poor to good, while the TSP measurement show a homogenous rock mass of average quality. Furthermore, in the prognosis the rock mass quality at area 7 is expected to be of good quality, however the TSP measurement show that the quality is only of slightly better quality than area 6. These results may however not be as accurate as the accuracy of the TSP measurements decreases as the distance from the tunnel face increases.

Table 14. Comparison between the rock classes found in the engineering geological prognosis and the interpretation of the TSP results at HT202.

Area	*Tunnel meter*	*Rock class prognosis*	*TSP interpretation*
2	12 584 – 12 610	Extremely poor (V)	Uncertain assessment due to influenced from tunnel. Tunnel face located at 12 592.
3	12 610 – 12 626	Very poor (IV)	Marginal improvement in rock quality compared to area 2. However, the rock quality is found to vary, meaning that a heterogeneous rock mass is expected.
4	12 626 – 12 643	Very poor (IV)	Homogenous area with worse rock mass quality than area 2 and 3.
5	12 643 – 12 682	Poor/Very poor (III/IV)	Heterogenous area with an overall better rock quality than area 4. Rock mass quality comparable to area 3.
6	12 682 – 12 719	Good/Poor (I/III)	Homogeneous area with average rock mass quality.
7	12 719 – 12 737	Good (I)	Area with better rock mass quality than area 6. However, the distance from the tunnel face is significant, meaning that assessment is uncertain. Possible influence from connections for bypass tunnels.

4.6. Comparison between TSP and geological mapping

A comparison between the generated TSP results and the results from the geological mapping was carried out to determine if the results coincide. The following sections include the comparison for each tunnel stretch.

4.6.1. Main tunnel, HT202

A comparison between the results generated from the TSP measurement and the geological mapping in the tunnel HT202 at Sätra-Kungshatt can be seen in Figure 16 and Table 15. In Figure 16 a comparison between V_p, V_s and the Q value can be seen, while in Table 15 a comparison between the rock classes found during the geological mapping and the interpretation of the TSP results can be seen. In both Figure 16 and Table 15 the results are divided into the areas of similar rock properties found from the TSP results. Overall, both similarities and discrepancies between the geological mapping and the TSP results can be seen. The largest discrepancy can be found in area 3 where the TSP results show a heterogenous rock mass of varying quality similar to area 2, while the geological mapping show a rock mass of extremely poor quality. In area 4 however, the TSP results predict a potential weakness zone which corresponds to the results from the geological mapping that show a zone of extremely poor and very poor rock mass. In area 5 both the TSP results and the geological mapping show a heterogenous rock mass of varying quality. In area 6 both methods show a homogenous area with similar properties to area 1.

It is important to note that even though similarities can be seen, the TSP results and the results from the geological mapping do not follow each other exactly. This can be noted in Figure 16 as the plots do not follow the exact same shape. An exact same shape in the plots is not expected as the methods measure different properties of the rock mass. The most important thing is that the results within the different areas show a similar trend, i.e. that the results from both methods show an increase, decrease or a mix of the two in the same area.

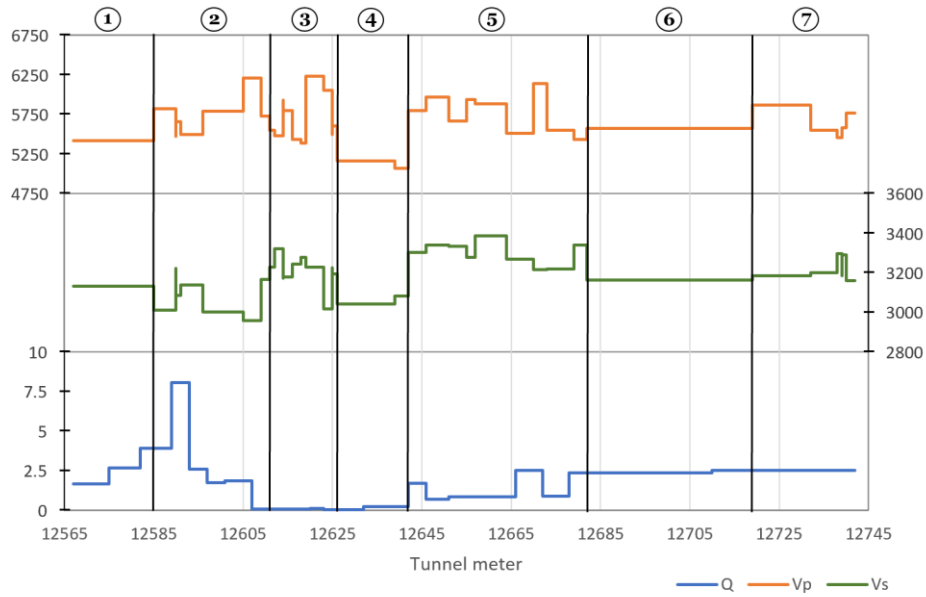

Figure 16. Comparison between the V_p, V_s and Q for the tunnel HT202. The results are divided into the different areas found during the analysis of the TSP results.

Table 15. Comparison between the rock classes found during the geological mapping and the interpretation of the TSP results at HT202.

Area	***Tunnel meter***	***Rock class mapping***	***TSP interpretation***
2	12 584 – 12 589	Poor (III)	Uncertain assessment due to influenced from tunnel. Tunnel face located at 12 592.
	12 589 – 12 593	Good/Acceptable (I/II)	
	12 593 – 12 597	Poor (III)	
	12 597 – 12 607	Poor/Very poor (III/IV)	
	12 607 – 12 610	Extremely poor (V)	

3	12 610 – 12 626	Extremely poor (V)	Marginal improvement in rock quality compared to area 2. However, the rock quality is found to vary, meaning that a heterogeneous rock mass is expected.
4	12 626 – 12 632	Extremely poor (V)	Homogenous area with worse rock mass quality than area 2 and 3.
	12 632 – 12 643	Very poor (IV)	
5	12 643 – 12 646	Poor (III)	Heterogenous area with an overall better rock quality than area 4. Rock mass quality comparable to area 3.
	12 646 – 12 666	Very poor (IV)	
	12 666 – 12 672	Poor (III)	
	12 672 – 12 678	Very poor (IV)	
	12 678 – 12 682	Poor (III)	
6	12 682 – 12 719	Poor (III)	Homogeneous area with average rock mass quality.
7	12 719 – 12 737	Poor (III)	Area with better rock mass quality than area 6. However, the distance from the tunnel face is significant, meaning that assessment is uncertain. Possible influence from connections for bypass tunnels.

4.6.2. Bypass tunnel, BP201

In Figure 17 and Table 16 a comparison between the results found from the geological mapping and the TSP measurement at BP201 is presented. The results are divided into areas based on the TSP results. Similarly to HT202, both similarities and discrepancies can be seen when comparing the TSP results with the geological mapping. In area 2 the TSP results predicts a potential weakness zone, which corresponds to the geological mapping as the rock mass was found to vary between poor and extremely

poor rock mass in this area. The same can be said for area 4 as a potential weakness zone was detected using TSP and the geological mapping show a rock mass that again ranges from poor to extremely poor rock mass. For area 3, the TSP measurements predict an increase in rock quality, while the geological mapping show a rock mass of similar rock quality to area 2 and 4. In area 5, TSP measurements show an increase in rock mass quality while the geological mapping found a rock mass of poor to very poor quality. In area 6 another discrepancy between the results can be seen as the TSP results show a decrease in rock mass quality while the geological mapping shows a significant increase in rock mass quality.

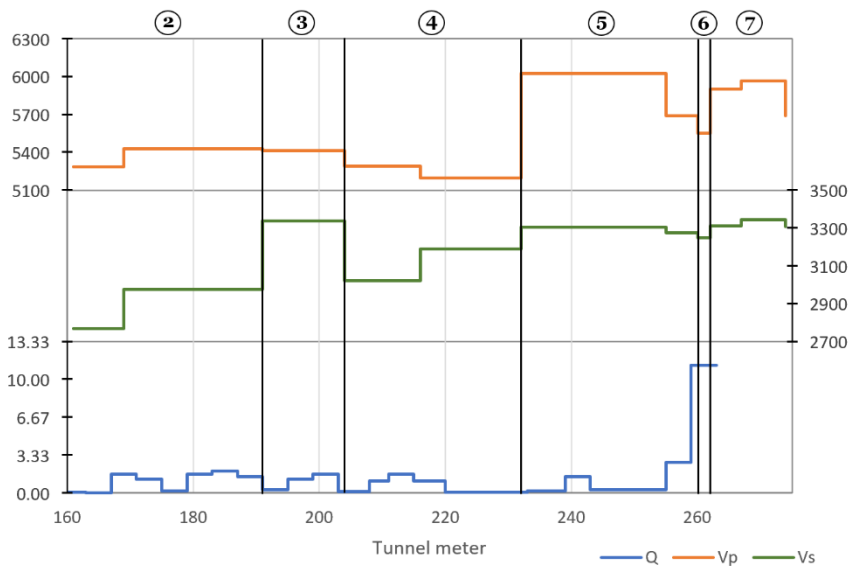

Figure 17. Comparison between V_p, V_s and Q for the tunnel BP201. Area 1 is not included since no data for the Q values was provided.

Table 16. Comparison between the rock classes found during the geological mapping and the interpretation of the TSP results at BP201.

Area	*Tunnel meter*	*Rock class mapping*	*TSP interpretation*
2	161 – 167	Extremely poor (V)	Weakness zone. Possible water bearing zone.
	167 – 175	Poor (III)	
	175 – 179	Very poor (IV)	
	179 – 191	Poor (III)	
3	191 – 195	Very poor (IV)	Increased rock stiffness.
	195 – 204	Poor (III)	
4	204 – 208	Very poor (IV)	Decreased rock stiffness. Weakness zone.
	208 – 220	Poor (III)	
	220 – 229	Extremely poor (V)	
	229 – 232	Poor (III)	
5	232 – 255	Very poor (IV)	Increased rock stiffness. More competent rock. Better rock mass quality than area 2, 3 and 4.
	255 – 260	Poor (III)	
6	260 – 262	Good (I)	Slight decrease in rock stiffness. Fair gneiss. Better rock mass quality than area 2, 3 and 4. Slightly worse rock mass quality than area 5.
7	262 – 274	N/A	Increased rock stiffness. Competent gneiss. Rock mass quality comparable to area 5.

4.6.3. Bypass tunnel, BP202

In Figure 18 and Table 17 a comparison between the results found from the geological mapping and the TSP measurement at BP202 is presented. The results are divided into areas based on the TSP results. As for the other tunnels, both similarities and discrepancies between the results can be seen in the comparison. In area 2 and 3 the TSP results show a decrease in rock mass quality, which corresponds to the geological

mapping as the rock mass was found to vary between very poor and extremely poor rock mass. For area 4 an increase in rock mass quality is expected and a rock mass of better quality than area 2 and 3 is expected. This somewhat corresponds to the geological mapping, however an area of very poor rock mass in the middle of area 4 was found, which was not indicated in the TSP results. In area 5 a decrease in rock mass quality is expected which also can be seen in the geological mapping. The TSP results does however show a rock mass of worse quality than area 2 and 3, which is not the case when looking at the geological mapping. For area 6, 7 and 8 the rock mass quality is expected to increase, while the geological mapping shows a heterogenous rock mass of varying quality. An increase in rock mass quality compared to area 2 and 3 can however be seen, which also is expected based on the TSP results.

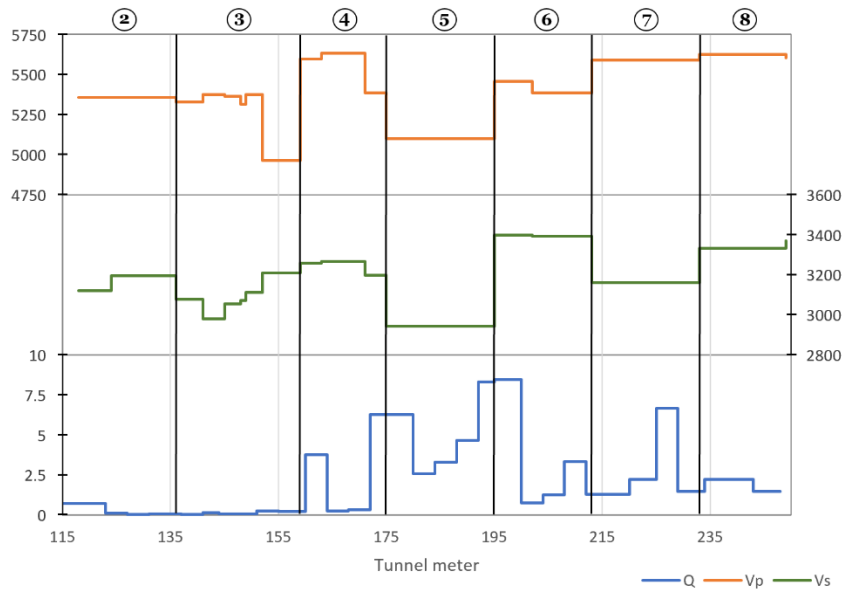

Figure 18. Comparison between V_p, V_s and Q for the tunnel BP202.

Table 17. Comparison between the rock classes found during the geological mapping and the interpretation of the TSP results at BP202.

Area	*Tunnel meter*	*Rock class mapping*	*TSP interpretation*
2	118 – 127	Very poor (IV)	Slight decrease in rock stiffness compared to area 1.
	127 – 136	Extremely poor (V)	
3	136 – 141	Extremely poor (V)	Further decrease in rock stiffness.
	141 – 144	Very poor (IV)	
	144 – 151	Extremely poor (V)	
	151 – 159	Very poor (IV)	
4	159 – 164	Poor (III)	Increase in rock stiffness. Better rock mass quality than area 1, 2 and 3.
	164 – 172	Very poor (IV)	
	172 – 175	Acceptable (II)	
5	175 – 180	Acceptable (II)	Decrease of rock stiffness. Worse rock mass quality than area 2 and 3. Could be possible weakness zone.
	180 – 192	Poor (III)	
	192 – 195	Acceptable (II)	
6	195 – 200	Poor (III)	Increase in rock stiffness. Comparable rock mass quality to area 2.
	200 – 204	Very poor (IV)	
	204 – 213	Poor (III)	
7	213 – 225	Poor (III)	Slight decrease in rock stiffness.
	225 – 229	Acceptable (II)	
	229 – 233	Poor (III)	
8	233 – 250	Poor (III)	Increase of rock stiffness.

4.7. Comparison between TSP and MWD

A comparison between the TSP results and the MWD results was carried out to determine if the two methods predict weakness zones or rock mass of lower strength in approximately the same locations in the tunnels. The following sections include a comparison between TSP and MWD for each of the analysed tunnels. The results are divided into areas based on the results from the TSP measurements, ie. the same areas as for the previous comparison between the geological mapping and the TSP results. The TSP results are presented in both a vertical and a horizontal point of view to easier be able to analyse the predicted weakness zones and their directions with regards to the tunnel. The TSP parameter presented is the calculated Dynamic young's modulus, which shows the stiffness of the rock. When the strength of the rock decreases, the stiffness of the rock should also decrease. The different reflectors and their directions are also displayed. For the MWD data, rock strength and degree of fracturing is presented.

4.7.1. HT202

In Figure 19 a comparison between the TSP results and the MWD results for the tunnel HT202 can be seen. Similarities between the results for the two methods can be seen in area 2, 4, 5, 6 and 7. In area 2 the MWD results show an area of lower rock strength which also can be seen in the TSP results. In area 4 both methods also show a potential weakness zone. In area 5, 6 and 7, the rock mass is expected to be of better quality than area 2, 3 and 4, which both methods show. In area 3 a discrepancy between the results can be seen as the MWD results show an area of lower rock strength while the TSP results do not. Many reflectors can however be found in this area indicting that a rock mass of varying quality is expected.

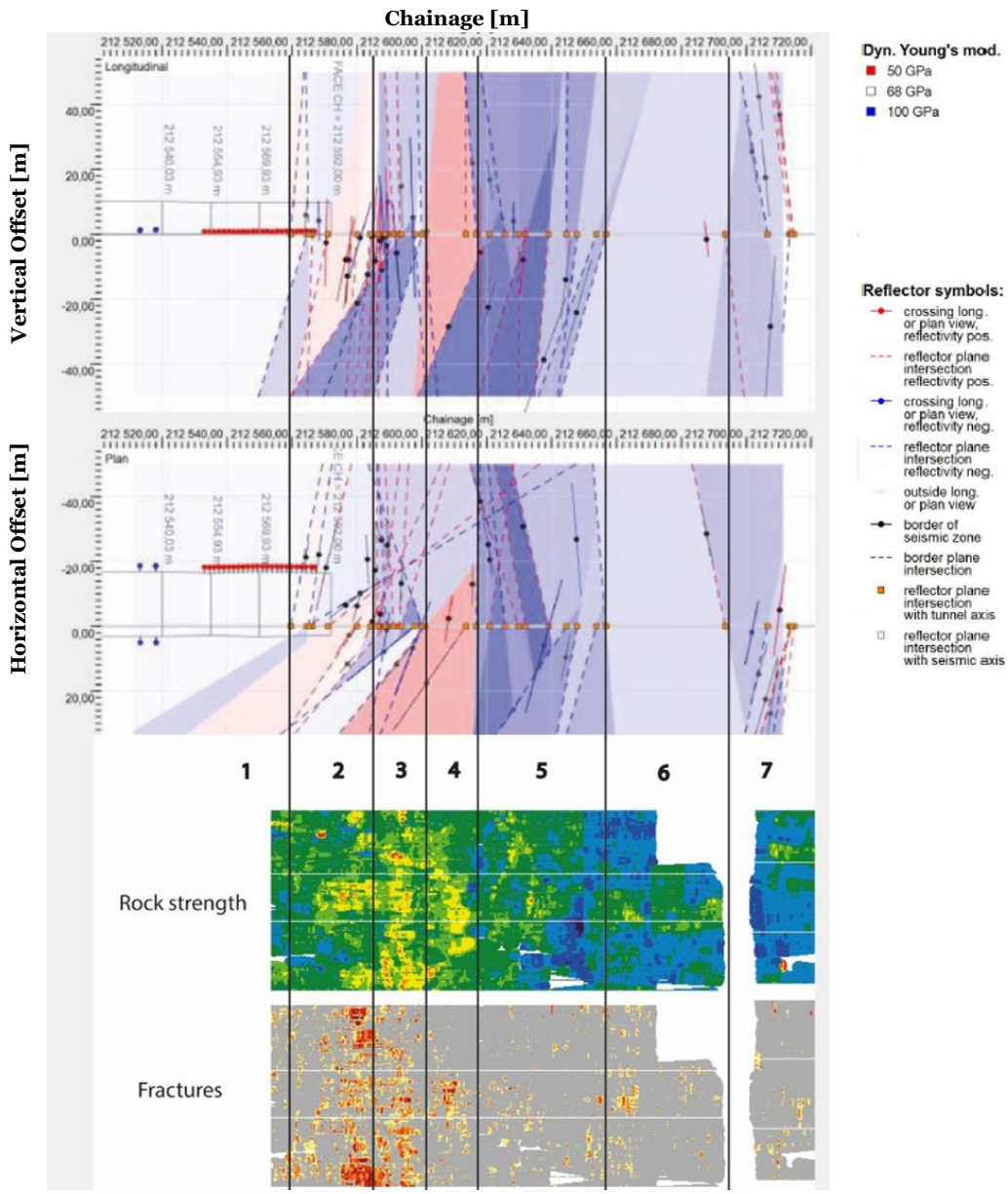

Figure 19. Comparison between the TSP results and the MWD results for the tunnel HT202. The TSP results are shown in the top two figures while the MWD results are shown in the bottom two figures. For the MWD measurements red, yellow, and light green indicates areas of lower rock strength. For fractures, a darker red indicates a higher degree of fracturing.

4.7.2. BP201

A comparison between the TSP results and the MWD results found at the tunnel BP201 can be seen in Figure 20. Discrepancies between the results for the two methods can mainly be found in area 2 and 5. This since the TSP results show a weakness zone in area 2 while the MWD measurements show a higher rock strength and lower degree of fracturing. In area 5 the TSP results show a rock mass of better quality while the MWD measurements show an area of lower rock strength in the middle of area 5. For areas 3, 4, 6 and 7, the results seem to align well.

4.7.1. BP202

In Figure 21 a comparison between the MWD results and the TSP results for the tunnel BP2020 can be seen. In areas 2, 3 and 5, potential weakness zones were identified for both TSP and MWD. In area 4 the TSP results show a slight increase in rock quality, while the MWD measurements show a slight increase in rock strength but a high degree of fracturing. For areas 6 and 7, an increase in rock strength is expected from the MWD results, which aligns well with the TSP results. However, a slight decrease in rock quality can be seen in the second half of area 6 which is not indicated in the MWD results.

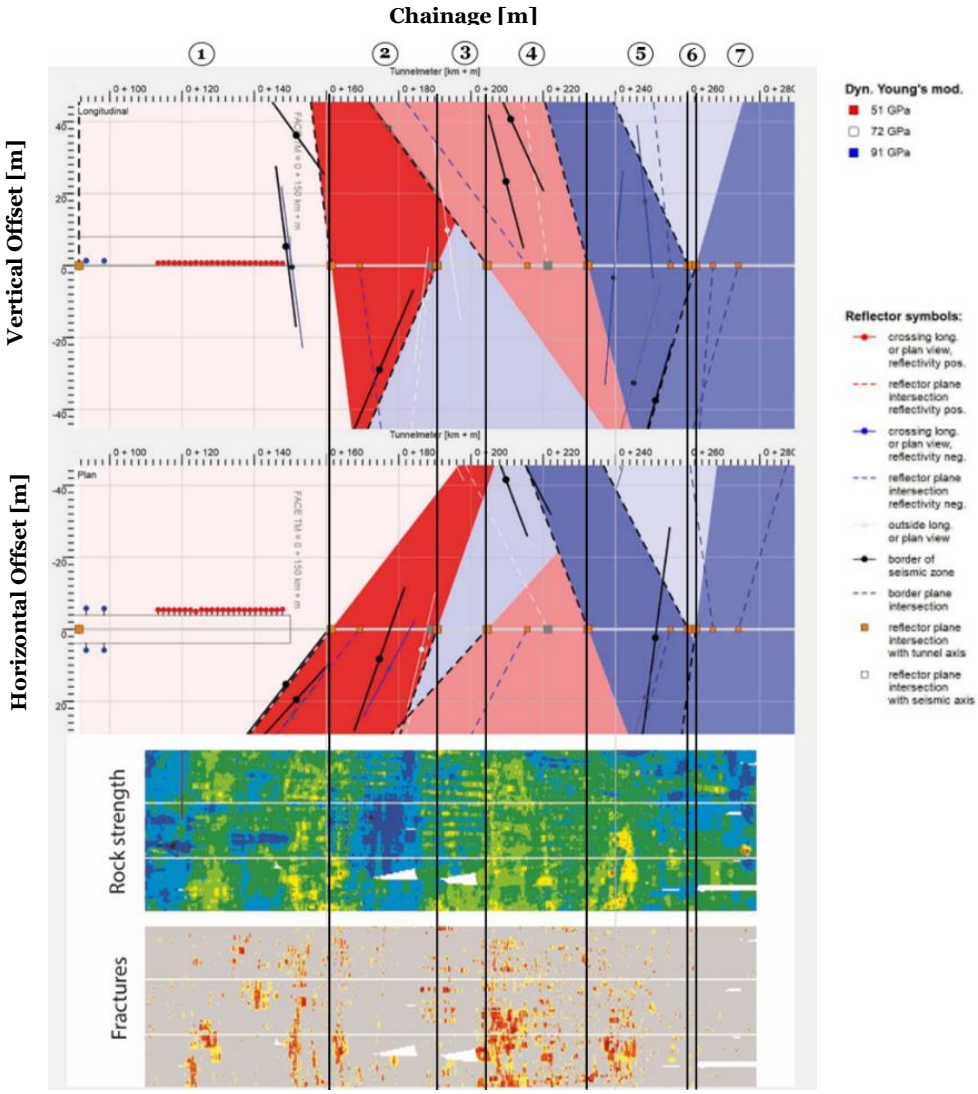

Figure 20. Comparison between the TSP results and the MWD results for the tunnel BP201. The TSP results are shown in the top two figures while the MWD results are shown in the bottom two figures. For the MWD measurements red, yellow, and light green indicates areas of lower rock strength. For fractures, a darker red indicates a higher degree of fracturing.

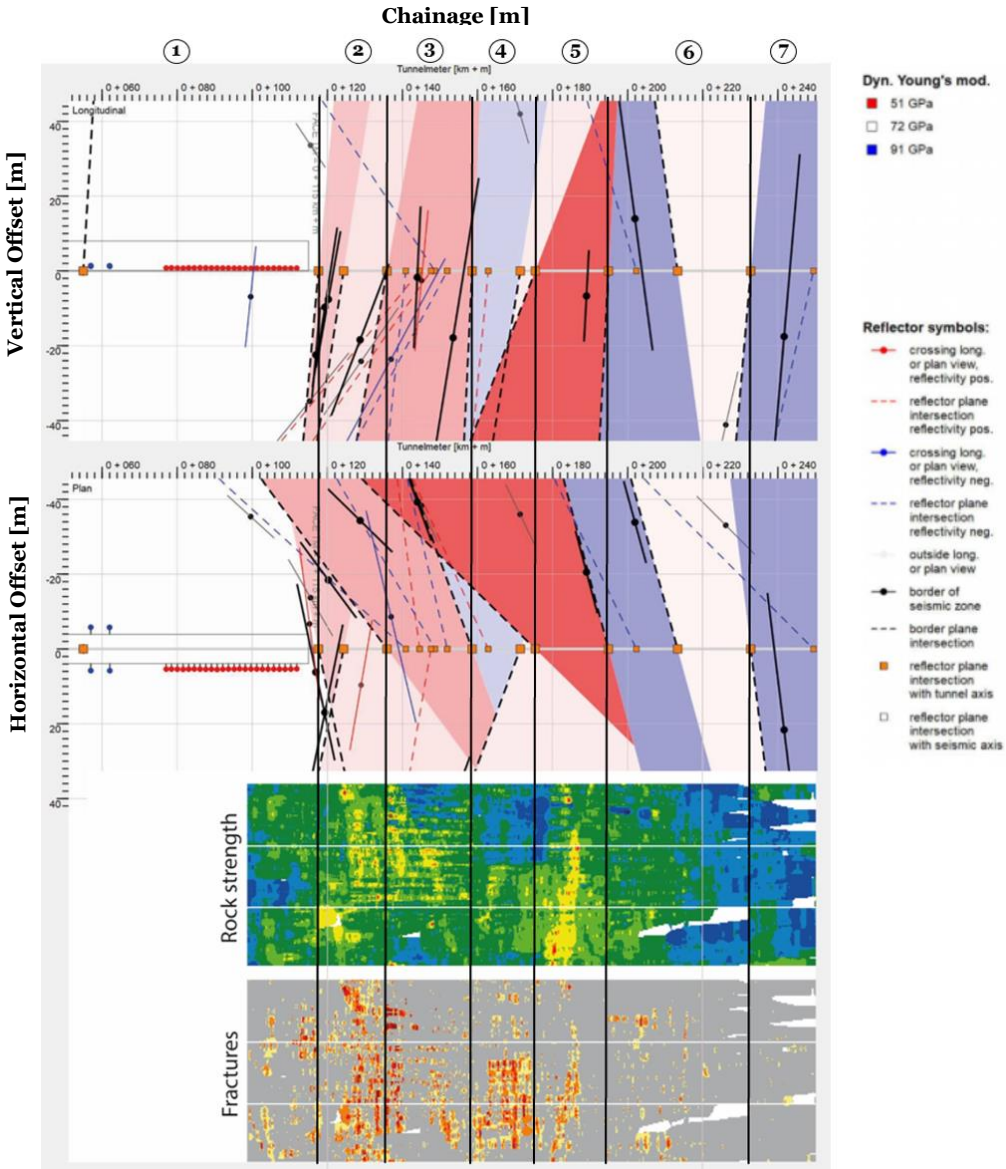

Figure 21. Comparison between the TSP results and the MWD results for the tunnel BP202. The TSP results are shown in the top two figures while the MWD results are shown in the bottom two figures. For the MWD measurements red, yellow, and light green indicates areas of lower rock strength. For fractures, a darker red indicates a higher degree of fracturing.

4.8. Statistical analysis

A regression analysis was carried out to determine if the results from the geological mapping correlate with the results from the TSP measurements. In Figure 22 and Figure 23 the analysis for the tunnel HT202 at tunnel meter 12 585 – 12 742 is shown. In Figure 22 the Q value retrieved from the geological mapping is compared to the primary wave velocity (V_p) retrieved from the TSP measurement, while in Figure 23 the Q value is compared to the secondary wave velocity (V_s). The R^2 value for the comparison between Q and V_p was found to be 0.0081 while the R^2 value for the comparison between Q and V_s was found to be 0.0368. Therefore, no linear correlation between the parameters was found at HT202.

In Figure 24 and Figure 25, the analysis for the bypass tunnel BP201 is presented. In Figure 24 the Q value is compared to the primary wave velocity (V_p) for the tunnel, while in Figure 25 the Q value is compared to the secondary wave velocity (V_s). The R^2 value for the comparison between Q and V_p was found to be 0.0921, while the R^2 value for the comparison between Q and V_s was found to be 0.1316. As for the tunnel HT202, no linear correlation between the parameters was found.

Finally, the analysis carried out for the bypass tunnel BP202 is presented in Figure 26 and Figure 27. In Figure 26 the Q value is compared to the primary wave velocity (V_p) for the tunnel, while in Figure 27 the Q value is compared to the secondary wave velocity (V_s). The R^2 value for the comparison between Q and V_p was found to be 0.0053, while the R^2 value for the comparison between Q and V_s was found to be 0.1588. As for the other tunnel stretches that were analysed, no linear correlation was found between the parameters.

As noted in the figures, V_p, V_s and Q values are compared. Investigation of how the six parameters ($\frac{RQD}{J_n}$, $\frac{J_r}{J_a}$, $\frac{J_w}{SRF}$) of Q corresponds to V_p and V_s were investigated but did not show any correlations and are therefore not included in the report. Values of the parameters are compiled in Appendix II. Lack of correlation can be related to the

limitations of TSP and the Q-system. The Q-system does not consider orientation or size of single fractures which could with significance impact V_p and V_s. This could imply TSP results to be a more accurate indication of joints and fractures than the Q-system.

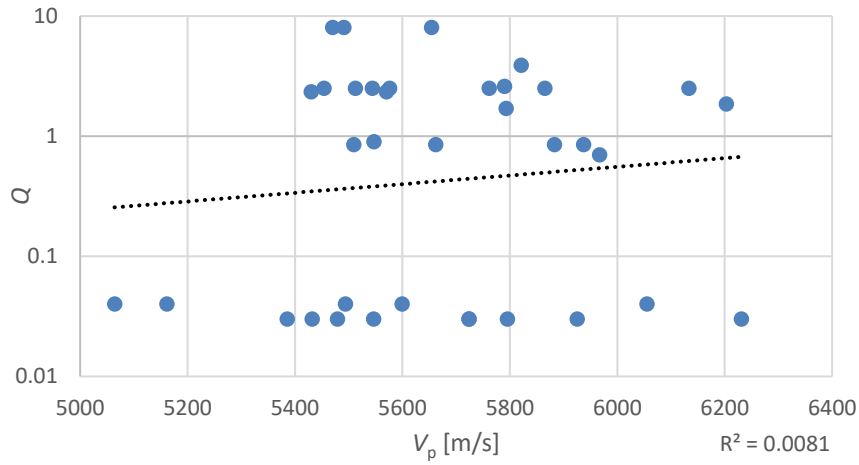

Figure 22. Regression analysis between the *Q* value retrieved from the geological mapping and the primary wave velocity (V_p) retrieved from the TSP measurement in HT202.

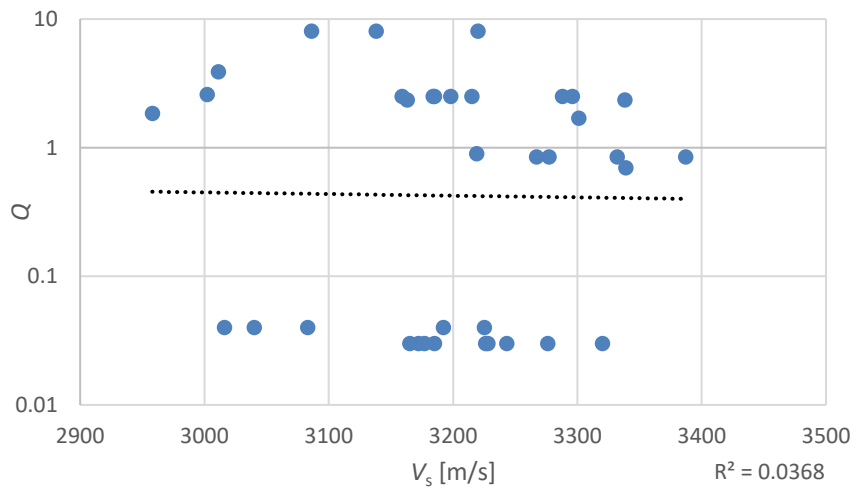

Figure 23. Regression analysis between the *Q* value retrieved from the geological mapping and the secondary wave velocity (V_s) retrieved from the TSP measurement in HT202.

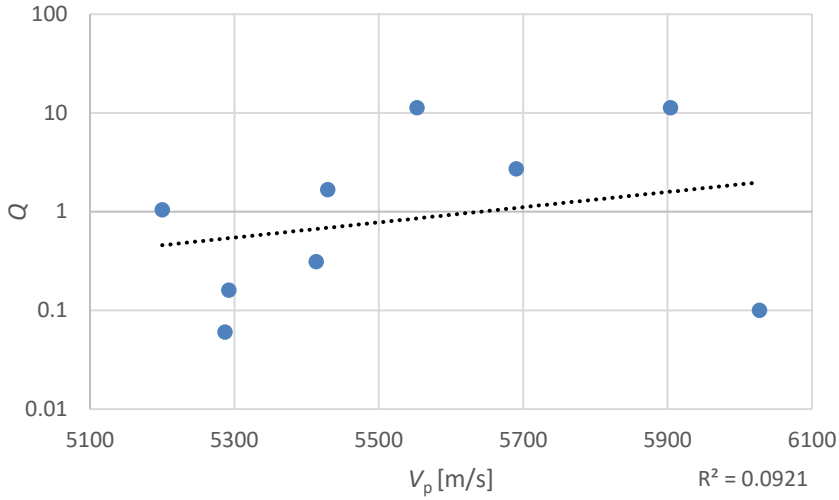

Figure 24. Regression analysis between the *Q* value retrieved from the geological mapping and the primary wave velocity (V_p) retrieved from the TSP measurement in BP201.

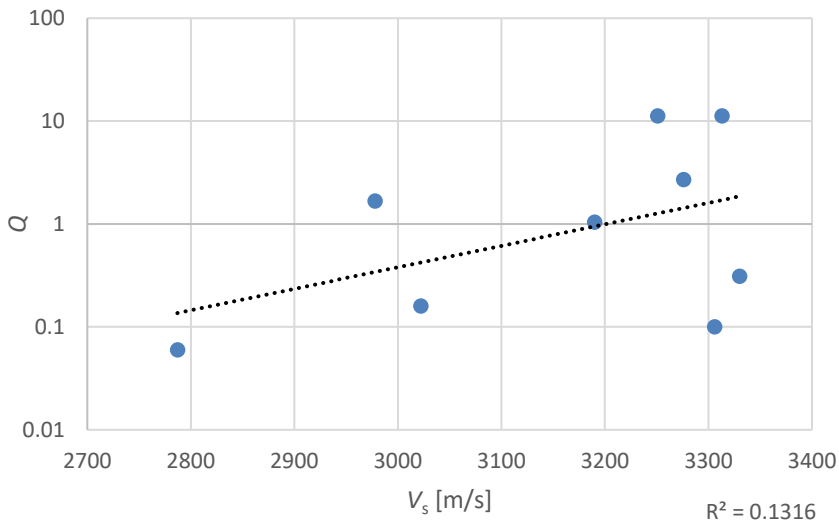

Figure 25. Regression analysis between the *Q* value retrieved from the geological mapping and the secondary wave velocity (V_s) retrieved from the TSP measurement in BP201.

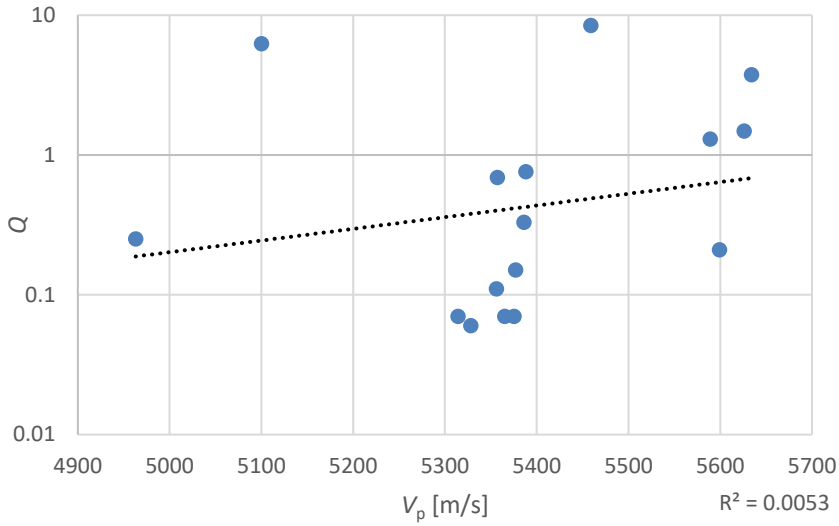

Figure 26. Regression analysis between the *Q* value retrieved from the geological mapping and the primary wave velocity (V_p) retrieved from the TSP measurement in BP202.

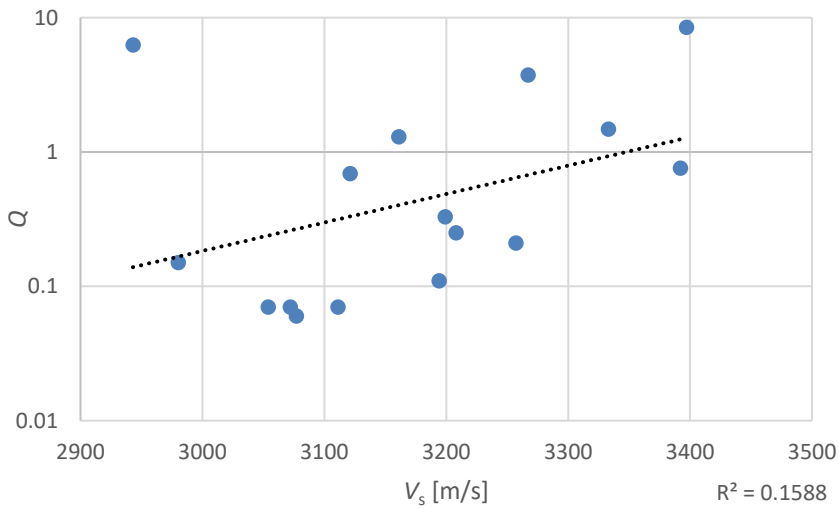

Figure 27. Regression analysis between the *Q* value retrieved from the geological mapping and the secondary wave velocity (V_s) retrieved from the TSP measurement in BP202.

4.8.1. Comparison with correlations from earlier work

By using derived V_p from TSP 303 with Barton (1991) relationship for $Q = 10^{(V_P - 3.5)}$ (Equation 5), his relationship for granite, $Q = (V_P - 3600)/50$ (Equation 7) and the Q-value from the geological mapping no correlation was found, see Figure 28, Figure 29 and Figure 30. Both suggested relationships did not in any way correspond close to the mapped value, maybe proving the complexity in interpreting TSP or the complexity in the geology itself.

The trend of the Q-value increasing with V_p does not apply for this case, meaning there are probably many other factors that must be affecting the Q-value besides V_p. Note that the difference in Q-value was not really affected by an increase of almost 1 km/s (going from 5064 m/s to 6203 m/s)

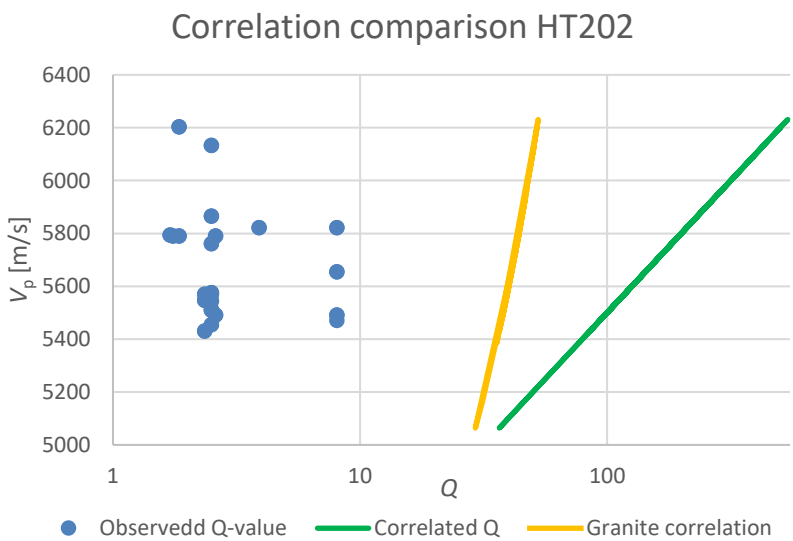

Figure 28. Derived Q-value for HT202 from using two suggested relationships by Barton (1991).

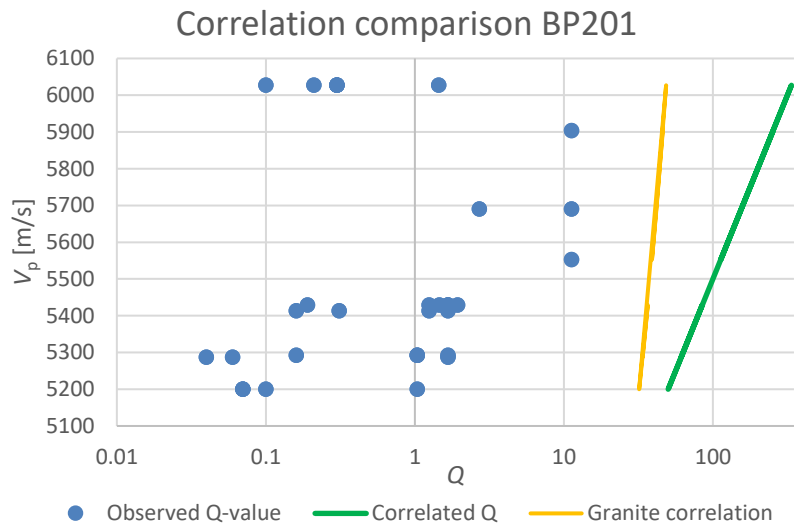

Figure 29: Derived Q-value for BP201 from using two suggested relationships by Barton (1991).

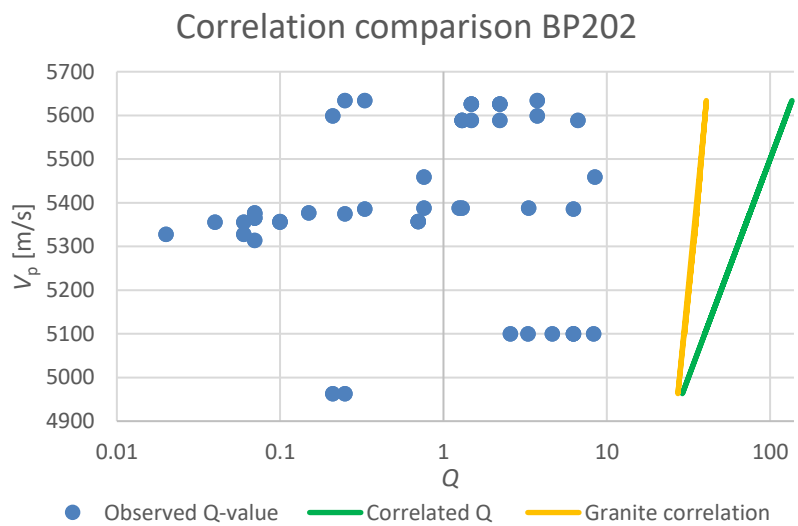

Figure 30. Derived Q-value for BP202 from using two suggested relationships by Barton (1991).

5. Discussion

As can be seen from the results, the TSP measurements have both strengths and weaknesses. When comparing the results from the geological mapping to the results from the TSP measurements, both similarities and discrepancies are observed. Overall, the results show that the TSP method is capable of detecting weakness zones in the rock. However, the results do not always show the true quality of the rock mass. This is to be expected as the method merely is used to provide an estimation of the rock quality ahead of the tunnel face. Many different factors can affect the results received from the TSP measurements, and often a lot of interpretation of the results is needed. Furthermore, the TSP method sometimes seemed to have a hard time detecting a few weakness zones that later were encountered during the excavation and geological mapping of the tunnels. This is especially relevant for BP201 and BP202 as some of the weaker zones in these areas were not detected using TSP. For HT202, the comparison between the TSP measurements and the geological mapping showed many similarities. However, the TSP method seemed to have a hard time detecting the lower rock quality in area 3. Many different reflectors were however encountered in this area which indicates that the area is of varying rock quality. The large number of reflectors may also be the reason for why a lower rock mass quality was not detected, as the zones of lower velocity may be hidden behind the other reflectors. Therefore, when encountering a zone with many reflectors, extra caution is necessary as the lower velocity zones may be hidden. The regression analysis performed showed that no distinct linear relation between the wave velocities and the Q value could be found.

As for the comparison between the geological mapping and the TSP results, the comparison between the engineering geological prognosis and

the TSP results showed both similarities and discrepancies between the results. The engineering geological prognosis expected the rock mass to be of poorer quality in areas 3 and 4 for HT202, while the TSP results only showed a weakness zone in area 3. The engineering geological prognosis did however expect the rock mass to be of good quality in areas 6 and 7, where the TSP results showed a rock mass of average quality. For these two areas the TSP results are more in line with the actual rock conditions than the engineering geological prognosis. This seems reasonable since the engineering geological prognosis is a mere prognosis.

When comparing the MWD results to the TSP results, many similarities between the results could be seen. The TSP results did generally show a lower rock mass quality in the same areas as the MWD results showed a lower rock strength. However, in some areas discrepancies could be seen. For some areas, the TSP method detected weakness zones that the MWD method did not and the other way around. An example is area 2 in BP201 where the TSP results predicted a weakness zone where the MWD results did not. When looking at the geological mapping for the same area, rock mass of extremely poor to poor quality could be found. Another example is area 5 in BP201 where the TSP results predicted an increase in rock quality, while the MWD results predicted a lower rock strength for parts of the area. The geological mapping here showed a rock mass of poor to very poor quality. It can therefore be noted that both the TSP method and the MWD method in some cases are capable of detecting weaker zones of the rock mass that the other method cannot detect. To reduce uncertainties regarding the quality of the rock mass, the methods can be used as complements to each other.

The geology in this part of the Stockholm Bypass project was found to be rather complex, with the rock mass quality being rather poor as the Q values typically were very low. This may be a reason for why the detection of weakness zones with the TSP system was not accurate in all places. As previously mentioned, the number of reflectors in one location might affect the TSP results. The TSP method might therefore be more suited

for less complex geology as often a smaller number of reflectors are encountered. A smaller number of reflectors also means less interpretation of the results. It can also be said that the TSP method might be better suited for detecting larger structures and not smaller variations in the rock mass as these are easier to distinguish. Larger variations in the quality of the rock mass may also make it easier to distinguish weakness zones as the wave velocity will have a larger range. The comparison of the actual Q values to the relationships suggested by Barton in Equation 6 and Equation 7 showed that the actual Q values in this case did not correspond to the suggested relationships. The reason for this can be that the Q values were too low, which further shows that the TSP method might be better suited in areas where the average rock quality is not as poor.

It is also important to note that most of the methods used are rather subjective and are often dependent on the observation or interpretation of the user. The TSP method requires interpretation of the results as an indirect parameter is measured and used to indicate the quality of the rock mass. For the geological mapping, the observations of the geologist performing the geological mapping is crucial for the results, and therefore different results can often be obtained from different people. It is therefore to be noted that when subjective methods are compared to each other it is difficult to determine what the correct or more accurate result may be.

For all methods, the execution of the measurement is crucial for the quality of the results. The results of the TSP measurements can for example be impacted by environmental factors such as noise. A complex geology may also be troublesome since it is hard to understand where not to trust TSP. Uncertainties in the TSP result can appear right in front of the tunnel face because of noise disturbance but also far ahead due to wave attenuation in the rock.

Finally, as noted above, the TSP method might not always provide an accurate result when it comes to determining the quality of the rock mass. However, the TSP method has proved that it, in many cases, can accurately detect potential weakness zones in front of the tunnel face even

though the regression analysis showed that there was no linear relation between the wave velocities and the Q value. The method can also be used to get a better understanding of the rock mass before excavation and provide a more detailed description of the rock mass than the engineering geological prognosis.

6. Conclusion and further research

From this thesis it can be concluded that:

- The TSP method is capable of detecting weakness zones in rock, however in some cases the accuracy is low.
- No correlation between the wave velocities and the Q value was found, however the results show that the TSP method can predict weakness zones.
- TSP might be better used in less complex geology and in areas where the contrast between rock mass quality is greater. This since the wave velocities will have larger range making it easier to distinguish weaker zones of rock mass from rock mass of good quality.
- The comparison between the suggested relationships for V_p and Q by Barton (1991) (Equation 6 and 7), and the actual Q values from the tunnels showed no relationship. A reason for this can be that the Q values from the actual tunnels are very low. This further indicates that the TSP method might be better suited for rock mass of not as poor quality.
- TSP and MWD can be used as complements to each other as the different methods sometimes detects weakness zones which the other method missed.
- No previous research could be found that shows a correlation between the Q value and the wave velocities derived from TSP.

Further research

No correlation between the Q values and the wave velocities could be found in this thesis. Since no previous research that show a correlation between the Q value and the wave velocities could be found, it is advised that more extensive research regarding the relationship between rock quality and the wave velocities is carried out. Since the Q system is not the only existing classification system, a relationship between the wave velocities and a different classification system might exist.

Since this case derived TSP results from a quite complex geology, with several weakness zones, further research is also suggested to investigate how TSP tends to respond to less complex geology. This to evaluate how much harder it is to interpret the TSP results in more complex geology. An ideal case with respect to Stockholm Bypass would be to compare these TSP results to results from TSP measurements in good or more intact granite or gneiss. This to evaluate if the TSP results from less complex geology are easier to interpret than for more complex geology.

Another suggestion is to investigate the interpretation of TSP results. Final TSP results, ready for interpreting are derived by filtering and processing raw TSP data using software Amberg TSP Ease. This process can be rather subjective and different final results could be produced depending on the software operator. It could therefore be of interest to evaluate how large the difference in the final results can be if the parameters are changed, or if a different filtering is used.

7. References

Alimoradi, A., Moradzadeh, A., Naderi, R., Salehi, M. Z., & Etemadi, A. (2008). Prediction of geological hazardous zones in front of a tunnel face using TSP-203 and artificial neural networks. *Tunnelling and Underground Space Technology , 23*, 711-717.

Almquist, R., & Hamrin, H. (1993). *Mechanized and automatic devices in drill rigs for long blast holes*. Luleå, Sweden : Proceedings Sec. Int. Symp. on Mine Mechanization and Automation.

Amberg Technologies. (2019). *Result Report: Tunnel Seismic Prediction - TSP 303 Plus, Campaign date: February 05, 2019, Face: bypass 202 TM 115 m, bypass 201 TM 150 m*.

Amberg Technologies. (2020a). TSP 303 Plus - Operation manual. *1.0*. Regensdorf, Switzerland: Amberg Technologies AG.

Amberg Technologies. (2020b). Amberg TSP Ease 1 - Evaluation manual. *1.0*. Regensdorf, Switzerland: Amberg Technologies AG.

Arghe, F. (2015). *E4 Förbifart Stockholm FSE209 Bergtunnlar Skärholmen Ingenjörsgeologisk prognos*. Stockholm: Trafikverket.

Barton, N. (1991). Geotechnical Design. *World Tunnelling*, 410-416.

Barton, N. (2002). Some new Q-value correlations to assist in site characterisation and tunnel design. *International Journal of Rock Mechanics and Mining Sciences, 39*(2), 139-286.

Barton, N. (2006). *Rock Quality, Seismic Velocity, Attenuation and Anisotropy*. London : CRC Press.

Barton, N., Lien, R., & Lunde, J. (1974). Engineering Classification of Rock Masses. *Rock Mechanics, 6*, 189-236.

Bieniawski, Z. T. (1989). *Engineering Rock Mass Classifications*. New York: John Wiley & Sons.

Choudhary, K., & Dickmann, T. (2019). 3D-Tunnel Seismic Prediction during tunnelling while underpassing an abandoned tunnel . *Tunnelling Asia*.

Deere, D. (1963). Technical description of rock cores for engineering purposes. *Felsmechanik und Ingenieurgeologie, 1*(1), 16-22.

Dickmann, T. (2014). 3D Tunnel Seismic Prediction: A Next Generation Tool to Characterize Rock Mass Conditions Ahead of the Tunnel Face. *Journal of Rock Mechanics & Tunnelling Technology, 20*(1), 35-47.

Dickmann, T., & Sander, B. K. (1996). Drivage-Concurrent Tunnel Seismic Prediction. *Felsbau, 6*, 406-411.

Dickmann, T., Hecht-Méndez, J., Rahbar, A., & Choudhary. (2016). Advanced seismic investigations during construction of hydro tunnels. *Recent Advances in Rock Engineering*, 149-157.

Dondurur, D. (2018). *Acquisition and Processing of Marine Seismic Data*. İzmir, Turkey: Elsevier Science. doi:10.1016/C2016-0-01591-7

Eidesen, J. M. (2013). *Metodikk for driving og sikring gjennom svakhetssoner ved Rogfast, Master's thesis*. Department of geology and rock mechanics. Trondheim: Norwegian University of Science and Technology.

Esmailzadeh, A., Mikaeil, R., Shafei, E., & Sadegheslam, G. (2018). Prediction of rock mass rating using TSP method and statistical analysis in Semnan Rooziyeh spring conveyance tunnel. *Tunnelling and Underground Space Technology, 79*, 224-230.

Gjelsnes, H. C. (2013). *Gjennomførbarhet for bruk av TBM ved Rogfast, Master's thesis*. Department of geology and rock mechanics. Trondheim: Norwegian University of Science and Technology.

Grüne-Yanoff, T. (2020). *Experiments, models and methodology*. Stockholm.

Higgins, M., & Segui, J. (2002). Blast Design Using Measurement While Drilling Parameters. *International Journal for Blasting and Fragmentation, 6*(3-4), 287-299.

Ignea, S. (2015). *Major Fracture Zones in Fiskarfjärden*. Department of Earth Sciences. Uppsala: Uppsala university.

Jianchun, L., Guowei, M., & Huang, X. (2010). Analysis of Wave Propagation Through a Filled Rock Joint. *Rock Mech Rock*(43), 789–798.

Kahraman, S. (2001). A correlation between P-wave velocity, number of joints and Schmidt hammer rebound number. *International Journal of Rock Mechanics & Mining Sciences*(38), 729–733.

Khandelwal, M. (2012). Correlating P-wave Velocity with the Physico-Mechanical Properties of Different Rocks. *Pure and Applied Geophysics*(170), 507–514.

Lausund, I. (2015). *Prognoser for stabilitet og sikring av svakhetssoner i Ryfylketunnelen, Masters thesis*. Institutt for geologi og bergteknikk. Trondheim: Norges teknisk-naturvitenskapelige universitet.

Li, S., Liu, B., Xu, X., Nie, L., Liu, Z., Song, J., Sun, H., Chen, L. & Fan, K. (2017). An overview of ahead geological prospecting in tunneling. *Tunnelling and Underground Space Technology, 63*, 69-94.

Li, S., Zhou, Z., Ye, Z., Li, L., Zhang, Q., & Xu, Z. (2015). Comprehensive geophysical prediction and treatment measures of karst caves in deep buried tunnel. *Journal of Applied Gepphysics, 116*, 247-257.

Lin, C., & Li, S. (2014). Tunnel Seismic Prediction (TSP) and its application in tunnel engineering. *Applied Mechanics and Materials*, 501-504.

Lindfors, U., Swindell, R., Rosengren, L., Holmberg, M., Sjöberg, J., Edelbro, C., Johansson, F. & Evins, P. (2019). *Projektering av bergkonstruktioner*. Trafikverket.

Lu, X., Liao, X., Wang, Y., Wang, G., Fu, Z., & Tai, H. (2020). The tunnel seismic advance prediction method with wide illumination and a high signal-to-noise ratio. *Geophysical Prospecting, 68*, 2444-2458.

Nordbø, K.-E. (2020). *Evaluation of potential of tunnel seismic prediction (TSP) for predicting engineering geological challenges for Rogfast subsea road tunnel, Master's thesis*. Department of Geoscience and Petroleum. Trondheim: Norwegian University of Science and Technology.

Otto, R., Button, E., Bretterebner, H., & Schwab, P. (2002). The application of TRT- true reflection tomography- at the Unterwald Tunnel. *Felsbau, 37*(2), 218-230.

Palmström, A. (2005). Measurements of and correlations between block size and rock quality designation (RQD). *Tunnelling and Underground Space Technology, 20*, 362-377.

Palmström, A., & Broch, E. (2006). Use and misuse of rock mass classification systems with particular reference to the Q-system. *Tunnelling and Underground Space Technology, 21*, 575-593.

Rai, P. S. (2015). An Overview on Measurement-While-Drilling Technique and its Scope in Excavation Industry. *Journal of The Institution of Engineers (India): Series D, 96*(1), 57-66.

Schunnesson, H. (1996). RQD predictions based on drill performance parameters. *Tunnelling and Underground Space Technology, 11*(3), 245-351.

Schunnesson, H. (1998). Rock characterisation using percussive drilling. *International Journal of Rock Mechanics and Mining Sciences, 35*(6), 711-725.

Schunnesson, H., & Sturk, R. (1997). *Drill Monitoring at the Hallandsås Project in Sweden*. Luleå, Sweden .

Selim, M. M., & Ahmed, M. K. (2006). Propagation and attenuation of seismic body waves in dissipative medium under initial and couple stresses. *Applied Mathematics and Computation, 182*(2), 1064-1074.

SGU. (2018). *Stockholmsområdets berggrund, jordarter, geologiska utveckling och erfarenheter från infrastrukturprojekt*. Stockholm : Sveriges geologiska undersökning. Retrieved from https://resource.sgu.se/produkter/sgurapp/s1808-rapport.pdf

SGU. (2020). *Byggnadsgeologi*. Retrieved from Svergies Geologiska Undersökning: https://apps.sgu.se/sgu3d/?page=byggnadsgeologi

Shi, S.-s., Li, S.-c., Li, L.-p., Zhou, Z.-q., & Wang, J. (2014). Advance optimized classification and application of surrounding rock based on fuzzy analytic hierarchy process and Tunnel Seismic Prediction. *Automation in Construction, 37*, 217-222.

Sjøgren, B. A. (1979). Seismic classification of rock mass qualities. *Geophysical Prospecting, 2*(27), 409-442.

Stille, H., & Palmström, A. (2003). Classification as a tool in rock engineering. *Tunnelling and Underground Space Technology, 18*(4), 331-345.

Telford, W. G. (1990). *Applied Geophysics* (2nd edition ed.). Cambridge: Cambridge University Press. doi:https://doi.org/10.1002/gj.3350270119

Trafikverket. (2019a). *Om E4 Förbifart Stockholm-projektet*. Retrieved February 8, 2021, from Trafikverket: https://www.trafikverket.se/nara-dig/Stockholm/vi-bygger-och-forbattrar/Forbifart-stockholm/Om-projektet/

Trafikverket. (2019b). *Så jobbar vi med berget i den södra delen*. Retrieved February 8, 2021, from Trafikverket: https://www.trafikverket.se/nara-dig/Stockholm/vi-bygger-och-forbattrar/Forbifart-stockholm/Tunnlar/tunnelbygge-och-geologi/sa-har-jobbar-vi-med-geologi/sa-jobbar-vi-med-berget-i-den-sodra-delen/

Trafikverket. (2020). *TSP undersökning FS2012600*.

Trafikverket. (2021). *E4 Förbifart Stockholm*. Retrieved February 8, 2021, from Trafikverket: https://www.trafikverket.se/nara-dig/Stockholm/vi-bygger-och-forbattrar/Forbifart-stockholm/

van Eldert, J., Schunnesson, H., Johansson, D., & Saiang, D. (2019). Application of Measurement While Drilling Technology to Predict Rock. *Rock Mechanics and Rock Engineering, 53*, 1349-1358.

Von, W., & Ismail, M. (2017). Evaluation of Tunnel Seismic Prediction (TSP) Result using the Japanese Highway Rock Mass Classification System for Pahang-Selangor Raw Water Transfer Tunnel. *AIP Conference Proceedings. 1892*. AIP Publishing LLC.

Wang, Z. (2001). Fundamentals of seismic rock physics. *Society of Exploration Geophysicists, 66*(2), 398-412.

Zhao, Y., Liu, H., Sun, Y., & Xiao, K. (2003). Research progress in tunnel geological prediction. *Progress in Geophysics, 18*(3), 460-464.

Appendix I – TSP data

The TSP data used in the thesis is presented below. The TSP data for the tunnel HT202 is presented in Table A1:1, while the TSP data for the tunnel BP201 is presented in Table A1:2. Finally, the TSP data for the tunnel BP202 is presented in Table A1:3.

Table A1:1. TSP data for the tunnel HT202.

Tunnel meter	V_p *[m/s]*	V_s *[m/s]*	***Poisson's ratio***	***Dynamic young's modulus*** *[GPa]*
initial	5416	3131	0.25	69
12 585	5821	3011	0.32	67
12 590	5470	3220	0.23	73
12 590	5654	3086	0.29	69
12 591	5491	3138	0.26	70
12 596	5790	3002	0.32	67
12 605	6203	2958	0.35	67
12 609	5724	3165	0.28	73
12 611	5546	3226	0.24	74
12 612	5479	3320	0.21	77
12 614	5925	3172	0.30	75
12 614	5724	3185	0.28	74
12 614	5795	3177	0.29	74
12 616	5432	3243	0.22	73
12 618	5385	3276	0.21	74
12 619	6231	3228	0.32	80
12 623	6055	3016	0.33	69
12 625	5494	3225	0.24	73
12 626	5599	3192	0.26	73
12 639	5161	3040	0.23	63
12 642	5064	3083	0.21	63
12 646	5793	3301	0.26	80
12 651	5967	3339	0.27	83

12 655	5662	3332	0.24	79
12 657	5937	3277	0.28	80
12 664	5883	3387	0.25	84
12 670	5509	3267	0.23	75
12 673	6133	3215	0.31	79
12 679	5547	3219	0.25	74
12 682	5430	3338	0.20	77
12 710	5570	3163	0.26	72
12 719	5865	3184	0.29	75
12 732	5544	3198	0.25	73
12 738	5454	3296	0.21	75
12 739	5512	3185	0.25	72
12 739	5576	3288	0.23	77
12 740	5761	3159	0.28	73

Table A1:2. TSP data for the tunnel BP201.

Tunnel meter	V_p *[m/s]*	V_s *[m/s]*	***Poisson's ratio***	***Dynamic young's modulus*** *[GPa]*
initial	5494	3176	0.25	71
161	5287	2769	0.31	54
169	5429	2978	0.28	63
191	5413	3330	0.20	76
204	5292	3022	0.26	63
216	5200	3190	0.20	68
232	6027	3306	0.28	82
255	5690	3276	0.25	77
260	5553	3251	0.24	75
262	5904	3313	0.27	81
267	5966	3344	0.27	83
274	5690	3310	0.24	79

Table A1:3. TSP data for the tunnel BP202.

Tunnel meter	V_p *[m/s]*	V_s *[m/s]*	***Poisson's ratio***	***Dynamic young's modulus*** *[GPa]*
initial	5527	3195	0.25	72
118	5357	3121	0.24	68
124	5356	3194	0.22	70
136	5328	3077	0.25	66
141	5377	2980	0.28	63
145	5365	3054	0.26	65
148	5314	3072	0.25	66
149	5375	3111	0.14	68
152	4963	3208	0.24	65
159	5599	3257	0.25	76
163	5634	3267	0.23	71
171	5386	3199	0.25	59
175	5100	2943	0.18	79
195	5459	3397	0.17	78
202	5388	3392	0.26	72
213	5589	3161	0.23	79
233	5626	3333	0.22	80
249	5604	3370	0.25	76

Appendix II – Data from geological mapping

The geological data used in the thesis is presented below. The geological data was retrieved from continuous geological mapping of the tunnels during excavation. In Table A2:1 geological data from the tunnel HT202 is presented, while in Table A2:2 geological data from the tunnel BP201 is presented. Finally, in Table A2:3 geological data from the tunnel BP202 is presented.

Table A2:1. Geological data from the tunnel HT202.

Tunnel meter	***RQD***	J_n	J_r	J_a	J_w	***SRF***	***Q***
12 567 – 12 575	60-80	9-12	1.5-2	6-8	1	1	1.0-2.3
12 575 – 12 582	65-70	9	1.5-3	4-6	1	1	1.4-3.9
12 582 – 12 589	70	9	2	4	1	1	3.9
12 589 – 12 593	65-75	6-9	2	2-4	1	1	3.6-12.5
12 593 – 12 597	60-65	9	2	4-8	1	1	1.6-3.6
12 597 – 12 601	55-60	9-12	1.5-2	4-6	1	1-5	0.2-3.3
12 601 – 12 607	50-55	9-12	2	4-8	1	1	1.0-2.7
12 607 – 12 620	20-40	12	1	6-8	1	5	0.04-0.08
12 620 – 12 623	40-55	12	1	8	1	5	0.1
12 623 – 12 632	15-30	12	1	6-8	1	5-10	0.02-0.06
12 632 – 12 642	35-50	9-12	1-1.5	8	1	1-2.5	0.15-0.3
12 642 – 12 646	60	12	2	6	1	1	1.7
12 646 – 12 651	50	12	1	6	1	1	0.7
12 651 – 12 666	60	9-12	1.5-2	4-6	1	2.5	0.8-0.9
12 666 – 12 672	60	9	1.5	4	1	1	2.5
12 672 – 12 678	60	12	1.5	8	1	1	0.9
12 678 – 12 710	60-90	4-12	1.5-2	4-6	1	1	1.1-3.6
12 710 – 12 742	80-85	4-9	2	4	1	1	1.5-3.5

Table A2:2. Geological data from the tunnel BP201.

Tunnel meter	***RQD***	J_n	J_r	J_a	J_w	***SRF***	***Q***
160 – 163	20	12	1	6	1	5	0.06
163 – 167	20	12	1	8	1	5	0.04
167 – 171	60	9	1.5	6	1	1	1.67
171 – 175	60	9	1.5	8	1	1	1.25
175 – 179	45	12	2	8	1	5	0.19
179 – 183	60	9	2	8	1	1	1.67
183 – 187	70	9	2	8	1	1	1.94
187 – 191	70	9	1.5	8	1	1	1.46
191 – 195	50	12	1.5	8	1	2.5	0.31
195 – 199	60	12	2	8	1	1	1.25
199 – 203	60	9	2	8	1	1	1.67
203 – 208	50	12	1.5	8	1	5	0.16
208 – 211	50	12	2	8	1	1	1.04
211 – 215	60	9	2	8	1	1	1.67
215 – 220	50	12	2	8	1	1	1.04
220 – 225	50	12	1	8	0.7	5	0.07
225 – 229	50	12	1	8	0.7	5	0.07
229 – 233	50	12	1	8	1	5	0.1
233 – 239	50	12	1	8	1	2.5	0.21
239 – 243	40-60	12	1-2	4-8	1	5	0.4-2.5
243 – 247	50-60	12	1-2	4-8	1	5	0.1-0.5
247 – 251	55-65	12	1-2	4-8	1	5	0.1-0.5
251 – 255	50-60	12	1-2	4-8	1	5	0.1-0.5
255 – 259	65	9	3	8	1	1	2.71
259 – 263	90	6	3	4	1	1	11.25

Table A2:3. Geological data from the tunnel BP202.

Tunnel meter	*RQD*	J_n	J_r	J_a	J_w	*SRF*	*Q*
115 – 119	50	9	1	8	1	1	0.69
119 – 123	50	9	1	8	1	1	0.69
123 – 127	30	9	1	6	1	5	0.11
127 – 131	20	15	1	6	1	5	0.04
131 – 135	25	15	1	6	1	5	0.06
135 – 141	10	12	1	8	1	5	0.02
141 – 144	35	12	2	8	1	5	0.15
144 – 147	35	12	1	8	1	5	0.07
147 – 151	35	12	1	8	1	5	0.07
151 – 155	40-65	12	1	8	1	2.5	0.2-0.3
155 – 160	50	12	1	8	1	2.5	0.21
160 – 164	45	6	2	4	1	1	3.75
164 – 168	45	9	2	8	1	5	0.25
168 – 172	60	9	2	8	1	5	0.33
172 – 176	75	6	2	4	1	1	6.25
176 – 180	75	6	2	4	1	1	2.57
180 – 184	70	9	2	4	0.7	1	3.57
184 – 188	60	9	2	4	1	1	3.3
188 – 192	50-75	9	2	3	1	1	3.7-5.6
192 – 195	75	9	2	2	1	1	8.3-8.33
195 – 200	70-90	6-9	2	2-8	1	1	1.9-15
200 – 204	55	9	1	8	1	1	0.76
204 – 208	60	9	1.5	8	1	1	1.25
208 – 212	60	9	2	4	1	1	3.33
212 – 216	70	9	1	6	1	1	1.3
216 – 220	70	9	1	6	1	1	1.3
220 – 225	80	9	1.5	6	1	1	2.22
225 – 229	80	6	2	4	1	1	6.67
229 – 234	80	18	2	6	1	1	1.48
234 – 239	80	18	2	4	1	1	2.22
239 – 243	80	18	2	4	1	1	2.22
243 – 248	80	27	2	4	1	1	1.48

TRITA-ABE-MBT-21509